10-4-2018 10:30 AM

Characterizing Ice-wedge Polygon Geomorphology in the Haughton Impact Structure, Devon Island

Jordan Hawkswell, *The University of Western Ontario*

Supervisor: Osinski, Gordon R., *The University of Western Ontario*

A thesis submitted in partial fulfillment of the requirements for the Master of Science degree in Geology

Abstract

Ice-wedge polygon networks are a common feature in periglacial environments formed through thermal contraction cracking and snowmelt infiltration. Polygons of similar morphology are ubiquitous throughout the mid-latitudes of Mars and are believed to have formed through thermal contraction processes. This study aims to characterize the polygons on Devon Island in the Canadian Arctic and the significant variations in geomorphology they display. The study uses LiDAR data to map, analyse, and compare three sites of polygonal terrain. Variations in polygon morphology such as size and orthogonality are observed in the relatively small study area. The results show that polygon morphologic variations in the High Arctic are linked mostly to substrate, stage of evolution and topographic factors. Insights into the factors that influence specific polygon morphology has implications for previous methods of predicting polygon morphology using factors such as homogeneity, and for variations of polygonal terrain in the mid-latitudes of Mars.

Keywords

Ice-wedge polygon, Periglacial, LiDAR, Polygon Distribution, Patterned Ground, High Arctic, Devon Island, Geomorphology, Permafrost, Mars

Co-Authorship Statement

Contributions to this thesis were made by Dr. Gordon Osinski, Dr. Etienne Godin, Dr. Michael Zanetti and Dr. Antero Kukko. Dr. Osinski and Dr. Godin provided comments and feedback on all chapters and figures. LiDAR data collection in the field and processing of raw LiDAR data was provided by Dr. Zanetti and Dr. Kukko.

Acknowledgments

Thank you to Gordon “Oz” Osinski and Etienne Godin for their mentorship and encouragement as supervisors throughout this project. This has been an extremely enriching experience and I am so grateful for the opportunity to have worked with you. Thank you to Mike Zanetti and Antero Kukko for strapping a LiDAR to their backs to scan the Arctic geomorphology, of which the resulting data is the foundation of this project. An extra thank you to Mike for taking time to teach me about LiDAR and how to process data in ArcGIS. Thank you to Colin Rowell for helping with Arctic grunt work. Thank you to Christy Caudill, Caitlin Watt, Sarah Simpson, Annika Van Kessel, Alyssa Werynski, Arya Bina, Matt Svensson, and the rest of the CPSX crew for support, skill sharing, climbing sessions, listening and for being great friends and colleagues. A special thank you to Patrick Ryan (and Mewtwo) for providing love and support through these two challenging years.

A huge thank you to Antero Kukko and the Centre of Excellence in Laser Scanning Research, Finnish Geodetic Institute for use of the KLS instrument vital to this project. Thank you to the Polar Continental Shelf Program for the support of our field work. Worldview high resolution imagery products were provided by Dr. John “Jack” Mustard.

Table of Contents

List of Tables

List of Figures

List of Abbreviations

Lcp……..……...Low centre polygon

Hcp……..……. High centre polygon

MGS……...……Mars Global Surveyor

MOC……...……...……Mars Orbital Camera

SPPA……...…...……Spatial Point Pattern Analysis

a.s.l……...……above sea level

LiDAR……...…..……Light Detection and Ranging

DTM ……...……Digital Terrain Model

KLS……...……Kinematic Mobile LiDAR Scanner

GPS……...……...……Global Positioning Device

GIS……...……Geographic Information Systems

HiRISE……...……...…High Resolution Imaging Science Experiment

Chapter 1

1 Background and Literature Review

The Canadian High Arctic contains a variety of geomorphological landforms formed as a result of the cold climate, seasonal temperature variations and permafrost ground. The freeze-thaw processes that occur in the permafrost throughout the region are often indicative of a periglacial environment and are important drivers shaping the periglacial landscape (Washburn 1980a). Devon Island (Fig. 1.1a), like much of the Canadian High Arctic, is located in the continuous permafrost zone (Zhang et al. 1999) and as such, contains an abundance of periglacial features. The specific region in west Devon Island where this study takes place is considered a polar desert climate (Lee and Osinski 2005). In addition to being cold with a mean annual air temperature of -16 °C, the region is very dry receiving little annual precipitation (~35 mm) (Lee and Osinski 2005). Devon Island is also the home of the Haughton impact structure (Fig. 1.1b), a well preserved 23.5 Ma impact crater (Young et al. 2013). The combination of a large impact crater, a cold, dry environment and a rich distribution of periglacial landforms in and near the crater makes for a quality Martian analogue for scientific study such as technology testing and geological analogue studies (e.g., Lee 1997; Pletser et al. 2009; Singleton et al. 2010; Haltigin et al. 2012).

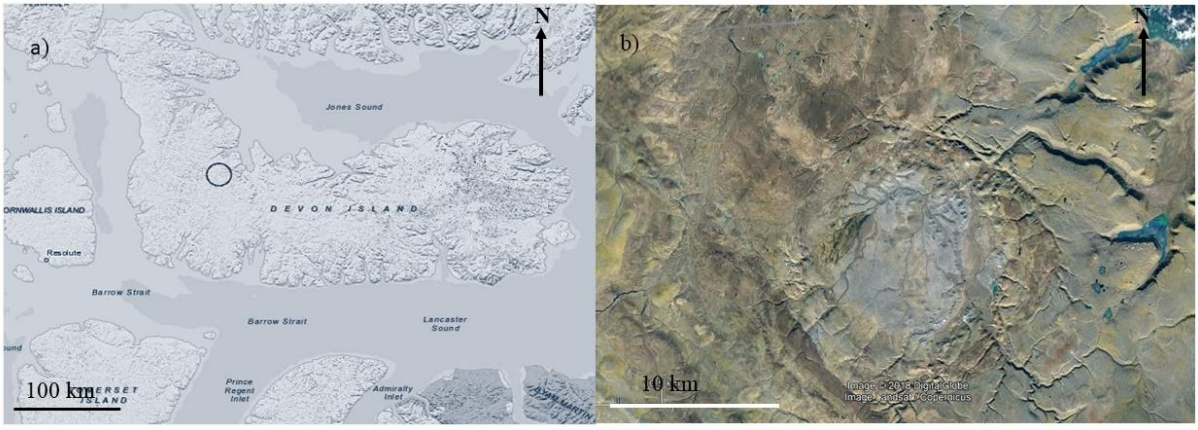

Figure 1.1: a) Devon Island, Nunavut with a circle indicating the location of the Haughton impact structure. b) A 2018 DigitalGlobe / Landsat / Copernicus image of the Haughton impact structure, the gray material being clast-rich impact melt rocks in the centre, surrounded by the crater rim (Google Earth 2018).

Polygonal terrain is a common periglacial feature throughout the Arctic region and is found within several units of unconsolidated sediments on Devon Island. Polygonal terrain is one of many forms of periglacial patterned ground that may occur in a periglacial environment, depending on terrain and climatic conditions (Washburn 1980a). Polygons are also ubiquitous throughout the mid-latitude regions on Mars (Mangold 2005; Levy et al. 2009), and their origins and formation have become a feature of great interest to planetary scientists due to their similarity to polygon terrain found on Earth (Fig. 1.2). Polygons on Mars suggests the presence of an ice-rich subsurface and thus, may aid in the study of ice distribution as well as past climatic conditions on Mars (Mellon 1997; Mustard et al. 2001; Head et al. 2003; Mangold 2005).

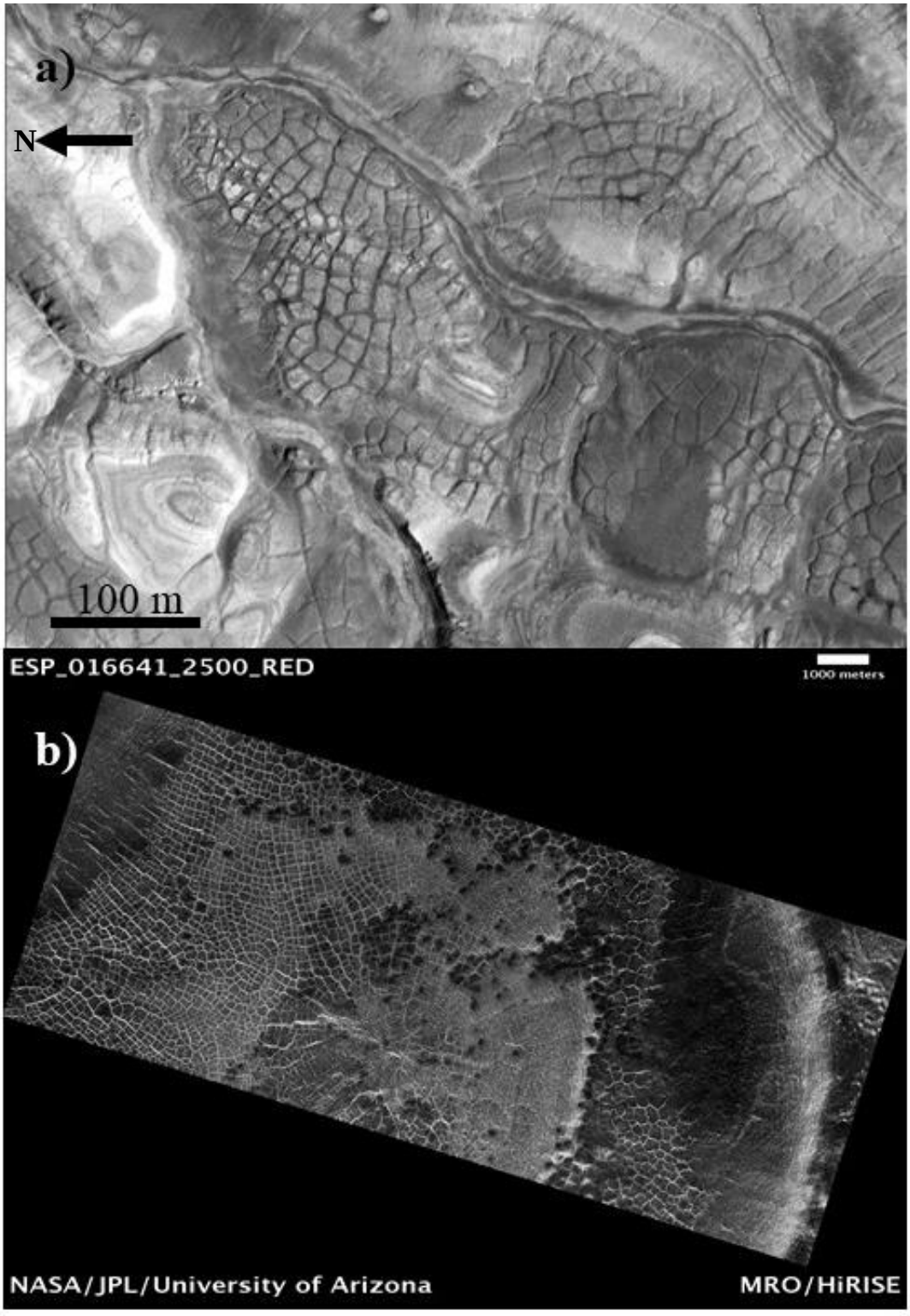

Figure 1.2: a) A WorldView 2013 image of polygonal terrain in the Haughton impact structure. b) A HiRISE image of polygon terrain in the northern hemisphere of Mars in Utopia Planitia (image from NASA/JPL/University of Arizona).

While the polar desert areas of Devon Island, such as the Haughton impact structure, are often used as a component for analogue studies, the controls and the characteristics of the polygonal terrain in the impact structure area remain somewhat under-studied. The purpose of this work is to determine the factors that contribute to polygon morphology in different sites within the polar desert environment of Devon Island, where climatic conditions are currently relatively constant. We aim to characterize the polygon terrain found in and around the Haughton impact structure and explore the drivers of the variations in the geomorphology of thermal contraction polygons within the study sites using both field surveying and remote sensing data interpretations. The findings of this study show that some polygon morphology is inconsistent with the literature, including the relationship of polygon morphology and substrate. However, some inconsistencies are supported by previous works with similar observations (e.g., Dutilleul et al. 2009; Ulrich et al. 2011; Haltigin et al. 2012). This work will contribute to the geomorphological studies of the High Arctic as well as the studies of polygons and the conditions of their formation in the context of Earth and Mars.

1.1 Permafrost and the Periglacial Landscape

The periglacial environment is described as one that is dominated by cold temperatures, permafrost and freeze-thaw action (Washburn 1980a; French 2007). When the periglacial concept was first introduced in the early 1900's, the definition of periglacial was linked to areas that closely bordered the Pleistocene ice sheets or glaciers (Lozinski 1909). Throughout a century of research, the definition of periglacial environments and the features unique to them has evolved and been refined. Currently, one of the most recognized definitions of periglacial has come to describe a range of cold-climate, non-glacial processes (Washburn 1980a; French 2007). Thus, the periglacial concept is no longer focused exclusively on areas adjacent to glacial landscapes by definition; however, they can be found in post-glacial environments (French 2000). Present day periglacial environments are typically found throughout the Arctic, in Antarctica, and in alpine environments at lower latitudes (Brown 1970; Washburn 1980a) although past periglacial environments and relict periglacial features have a wider range (e.g., Bertran et al. 2017).

1.1.1 Permafrost

Permafrost is a significant component of a periglacial environment and crucial to the formation of several periglacial landforms. Permafrost is defined as ground material that has a mean annual surface temperature that remains at or below 0°C for two or more consecutive years and is determined exclusively by temperature. (MacKay 1972; French 2007; Dobiński 2011).

Figure 1.3: Circumpolar map of the distribution of permafrost in North America. After the International Permafrost Association (1998).

Permafrost extends throughout much of the Arctic region in what is known as the continuous permafrost zone (Fig. 1.3), an area where permafrost is ubiquitous under all land surface except where new sediment has been recently deposited (Brown 1970). The continuous permafrost zone can range in thickness from over 450 m in the high-latitudes of North America, with reports of over 1000 m in Siberia, to ~30–60 m in the southern reaches of continuous permafrost (Brown 1970; Washburn 1980b; van Everdingen 1998; French 2007). Permafrost distribution is fragmented in the discontinuous permafrost zone (Fig. 1.3) where permafrost is present under some land surfaces and not present in other areas. Permafrost depth can range from ~60 m to a few centimetres in southern areas of the discontinuous permafrost zone (Brown 1970; French 2007). Permafrost distribution is dependent primarily on latitude and altitude, with higher latitudes and altitudes more likely to be within the continuous permafrost zone. Other factors, such as the n-factors which is the ratio of degree-day sums at the ground surface to the degree-day sums of the air at a standard height (Klene et al. 2001), also affect permafrost conditions (Brown 1970; Dobiński 2011). Much of the High Arctic typically lies within the continuous permafrost zone (Fig. 1.3). Above the permafrost is a layer known as the active layer which thaws in the warmer months of summer and freezes again in the winter (Brown 1970). The active layer is a dynamic zone that will range in thickness year to year depending on local factors such as air temperature, snow cover, vegetation and ground material (French 2007).

Permafrost is a key component of a periglacial environment and creates a base on which many periglacial features form from freeze-thaw processes (Washburn 1980a). Periglacial features shape the frozen landscape and provide insight into the processes that formed them.

1.1.2 Periglacial Geomorphology

Periglacial geomorphology is a subset within geomorphology that aims to study periglacial features and landscapes and how they may change over time. Geomorphology is the study of landforms and their origins as well as their relation to the geologic and geographic setting. Periglacial geomorphology is specific to present or past cold environments and

their landforms that are strongly influenced by frost action and the presence of permafrost over time (Washburn 1980a; Thorn 1992). In this case, the periglacial focus includes processes and the resulting landforms in cold environments not covered by glaciers in the Arctic, Antarctic and high-altitude environments at lower latitudes (Bursch 1993). The influence of ground ice and permafrost on the development of periglacial landforms is crucial to consider in periglacial geomorphology (Thorn 1992); however, ground ice does not always indicate periglacial processes and geomorphology (Washburn 1980a; Bursch 1993). Factors such as climate, geology and hydrology can have a strong influence on the formation of periglacial landforms and are also important to consider in periglacial geomorphology (French 2007).

1.1.3 Periglacial Features

A significant part of the periglacial environment are the surface features associated with the freeze-thaw processes that are widespread, as well as permafrost and subsurface ice. Periglacial surface features are varied and include a range of landforms including thermokarst (Washburn 1980a; Kokelj and Jorgenson 2013), pingos (Müller 1959; MacKay 1962), sorted patterned ground (Uxa et al. 2017) and thermal contraction polygons (Lachenbruch 1962; Black 1976) (Fig. 1.4).

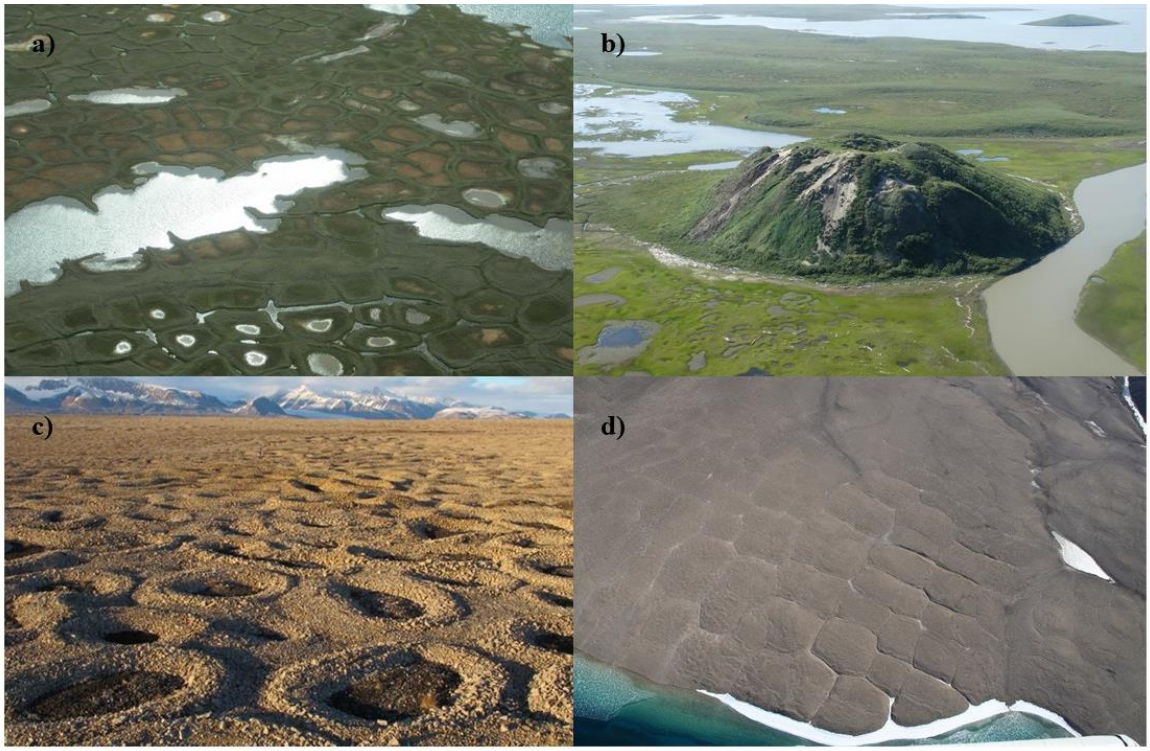

Figure 1.4: a) Thermokarst processes forming lakes and ponds in Alaska (polygons ~30 m across) (USGS). b) A large (~120 m long) pingo in Tuktoyaktuk (Adam Jones, Ph.D./Global Photo Archive/Flickr). c) Sorted circle patterned ground (~1 m across) in Svalbard, Norway (Bernard Hallet 2013). d) High-centred thermal contraction polygons (~ 50 m across) outside of the Haughton impact structure, Devon Island.

Thermokarst refers to the processes of, and landforms that result from, thawing permafrost and the melting of ground ice (Kokelj and Jorgenson 2013). Thawing can be brought on by physical disruption to the permafrost thermal equilibrium such as a sudden change in surface conditions, vegetation growth, or from changes in climate such as increases in air temperatures (Washburn 1980a). Thermokarst includes numerous features such as lakes (Fig. 1.4a) and pits that form in degrading permafrost, which processes are discussed in detail by Jorgenson and Osterkamp (2005).

Pingos are hill-like features (Fig. 1.4b) covered with soil and vegetation that contain an ice core that forms and grows slowly in permafrost environments (Brown 1970; Mackay

1987). Pingos can develop for hundreds of years and grow to be over 30 m in height and 400 m in length (Brown 1970). A pingo ice core is formed in either an open system or a closed system, both impacting their respective groundwater availability (Mackay 1962, 1979). Over time, pingos may crack along the top and eventually collapse due to mechanical failure or thermal disturbance of the permafrost (Brown 1970; Mackay 1987).

Patterned ground can refer to an array of landforms observed on the periglacial surface that displays geometric morphology. These landforms are referred to be either sorted or non-sorted (Washburn 1980a). Sorted patterned ground is defined by soil materials organized by their grain-size due to frost action and freeze-thaw processes. This type of patterned ground takes on geometric forms such as circles (Fig. 1.4c), polygons or stripes (Washburn 1956; Treml et al. 2010, Feuillet et al. 2012). It is generally accepted that clasts are moved through the permafrost active layer by frost action and thermal gradients to the outer edges of the form; however, the exact mechanisms for all cases of sorting are not well constrained (Washburn 1956; Kessler and Werner 2003; Feuillet et al. 2012; Ballantyne 2013). Intense frost action causes similarly sized materials being sorted together creating a centre of one sized material that is bound by clasts of a different size (Washburn 1956, 1980; Kessler and Werner 2003). The sorted patterned ground often occurs in nets of many individual polygons, circles or stripes across an area. Sorted circles and polygons typically occur on flat surfaces while stripes will occur on slopes (Washburn 1956). Non-sorted patterned ground also often takes on geometric forms such as circles, stripes and polygons however they lack borders of stones and instead may be bordered by vegetation (Washburn 1956, 1980; Brown 1970). Non-sorted polygons are commonly bordered by a crack with furrowed rims and may be of thermal contraction origins (Washburn 1980a). One prominent and one of the most widespread forms of non-sorted patterned ground is the ice-wedge polygon due to thermal contraction (Fig. 1.4d) (French 2007).

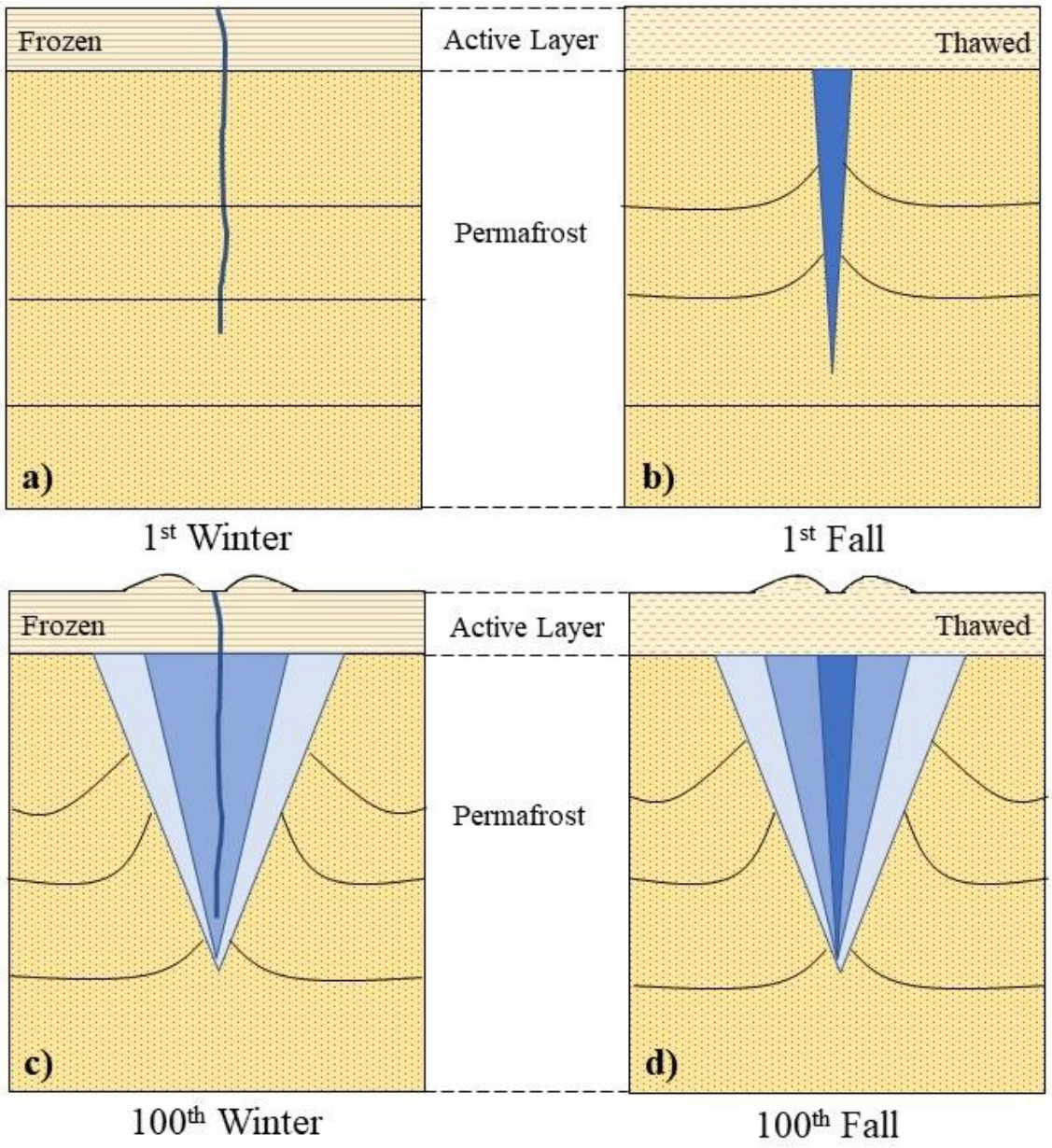

Figure 1.5: Diagram showing the initiation of an ice-wedge by cracking in the winter (a) and growth of ice-wedge by an infill of water and subsequent freezing in the fall (b). Ice-wedge growth continuing by contraction cracking over time is shown in (c) and (d), with a slight upward movement of sediment shown that contributes to raised rims around the trough. Modified from Lachenbruch (1962).

Thermal contraction polygons are formed by networks of contraction cracks extending through frozen ground. Cracks are initiated by stresses in permafrost or frozen ground (Fig. 1.5a) from a rapid decrease in air temperature (Lachenbruch 1962). Initial contraction crack widths are typically on the order of >1 cm and depth are on the order of 1–5 meters into the permafrost (Mackay 1974, 1999; Mackay and Burn 2002; French 2007). Contraction cracks may occur in a singular crack or as a point that has contraction cracks radiating from it, usually three cracks at 120º intervals. Over time, multiple contraction cracks may intersect to create large networks of polygons. Singular cracks may intersect to form X-shaped intersection creating an orthogonal network (Fig. 1.6) where most intersections are at ~90º (Washburn 1980; French 2007). A network primarily containing intersections with cracks radiating at 120º with form a non-orthogonal network (Fig. 1.6) (French 2007). Depending on the material infilling the contraction cracks, such as fine sediments or water, thermal contraction polygons can be labelled as either ice-wedge or sand-wedge polygons (Washburn 1980a).

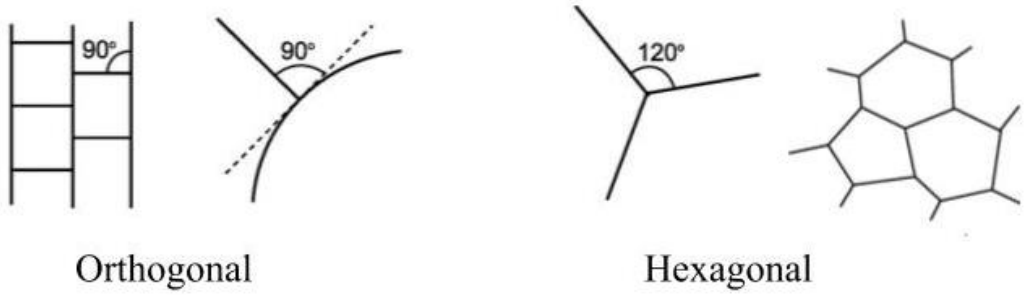

Figure 1.6: An example of orthogonal and non-orthogonal (hexagonal) networks. Modified from French (2007).

Following the opening of a crack due to contraction, an ice-wedge will form when temperatures rise in the spring and contraction cracks infill with meltwater, which will refreeze when it hits the permafrost below the active layer (exaggerated in Fig. 1.5b). The cracks are forced open with the expansion of water at it freezes. The process of cracking, water infill and freezing can occur several times a year and over hundreds of years to form thick wedges of ice after repeated cracking in the same location (Fig. 1.5c, d) (Lachenbruch

1962; Mackay 1993; Fortier and Allard 2005). With the right conditions ice wedges can continue to grow and become very thick, however, once the tensile strength of an ice-wedge becomes more than the stresses of the frozen ground growth will stop and the ice-wedge will remain mostly stable in size until conditions change (Lachenbruch 1962). Networks of ice-wedges form ice-wedge polygons that may range in size across terrestrial landscapes from 15–40 m in diameter (French 2007). The same cracking and infilling process can also occur with sand or other debris to form sand-wedge polygons in environments that are more arid (Black 1976; Mellon et al. 2014).

Ice-wedge polygons consist of a centre and the ice-wedge filled contraction cracks that surround the centre. The growth of an ice-wedge pushes material from the edges towards the center of the polygon as the growing wedge displaces sediment (Mackay 2000; French 2007). There is also a lateral movement of sediments due to thermal expansion of sediments from the centre of the polygon to the sides (Mackay 1980, 2000). The combination of these two factors creates a raised rim along the ice-wedge crack (Fig. 1.7b) making the polygon center appear lower relative to the raised rim. This morphology is known as a low-centred polygon (lcp) (Fig. 1.7b). When ice-wedges around a lcp begin to degrade, they leave behind sunken troughs and the polygon centers may consequently appear raised above the contouring trough. Polygons with this morphology are known as a high-centred polygon (hcp) (Fig. 1.7c) (Washburn 1980a; Mackay 2000). If ice-wedge development and sediment transport have not yet raised the rims of the contraction crack the polygon is considered flat (Fig. 1.7a) (Mackay 2000).

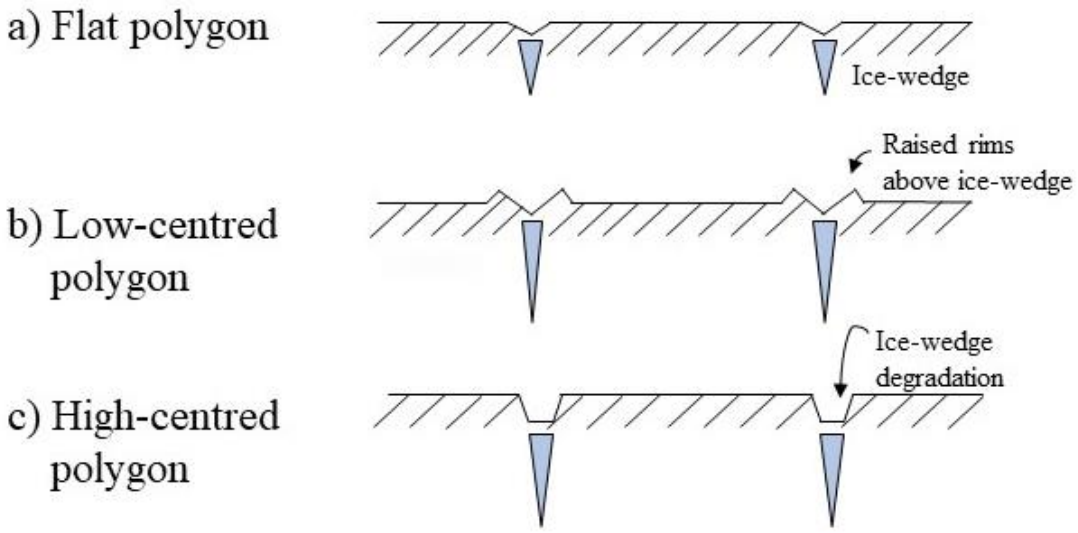

Figure 1.7: a) Profile of a flat ice-wedge polygon morphology with ice wedges shown beneath the surface. b) Profile of low-centred polygon morphology with raised rims above the ice-wedges. c) Profile of high-centred polygon morphology showing ice-wedge degradation and raised centre. Modified from Mackay (2000).

Ice-wedges may be further categorized as epigenetic, syngenetic or antisyngenetic (Fig. 1.8) relative to the surface around them (Mackay 1990, 2000). Epigenetic ice wedges (Fig. 1.8a) normally occur in flat areas that are relatively stable, having no significant erosion or accumulation of materials. These ice-wedges are younger than the material around them and continue to widen over time but not deepen, pushing material to the trough rims. (Mackay 1990; French 2007). The troughs develop rims on either side creating a distinctive epigenetic profile (Mackay 1990; French 2007). Syngenetic ice-wedges (Fig. 1.8b) occur where ground material is accumulating, often at the base of slopes, in floodplains or where peat is accumulating (Mackay 2000; French 2007). New layers of sediment deposited on top of existing ice wedges causing the ice-wedge to grow upwards with new cracking and infilling. This action makes the ice-wedge relatively deeper over time. The ice-wedge may be thin if there is a high amount of sediment accumulating above it and growth is mostly

upward but may grow thicker if sediment accumulation is lower and growth can go both upward and outward (Mackay 1990; French 2007).

Antisyngenetic ice-wedges (Fig. 1.8c) form where there is ground erosion and the tops of ice-wedges may degrade away, typically on slopes (Mackay 2000). As material erodes and the top of the ice-wedge becomes degraded the ice-wedge also becomes relatively shallower. New cracks form deeper into the ground creating downward and outward growth of the ice-wedge (MacKay 1990; French 2007). The focus of this work is on epigenetic ice-wedges that occur in pre-existing permafrost in relatively flat areas with no major erosion or accumulation of sediments. This type of polygon is the most common and, based on surface observation, the most similar to the polygons observed in the mid-latitudes of Mars where there is less significant erosion or accumulation of ground material.

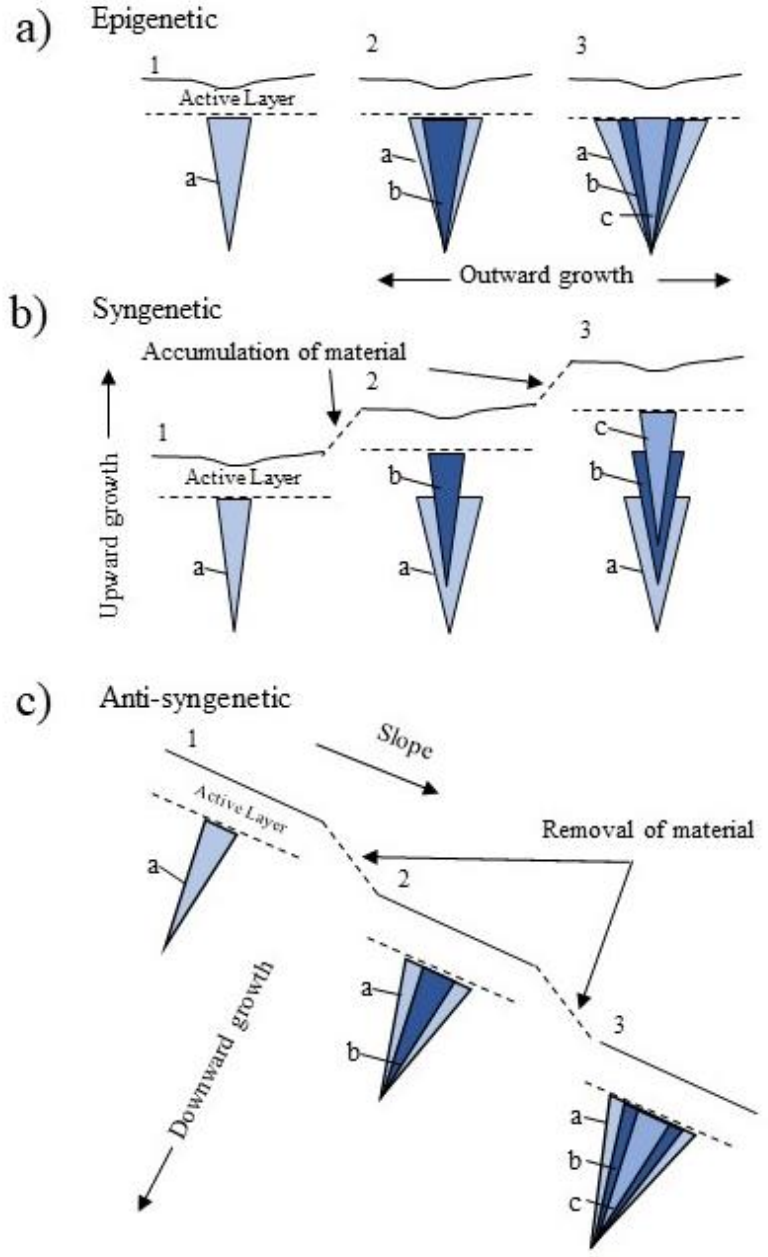

Figure 1.8: a) Epigenetic ice-wedge growth on a flat surface with overall outward growth. b) Syngenetic ice-wedge growth on a flat surface with accumulation of material and overall upward growth. c) Anti-syngenetic ice-wedge growth on a slope with the removal of surface material and overall downward growth. Modified from Mackay (1990).

The study of periglacial geomorphology is used to learn about current, past, and future environments, both on Earth and Mars. The features observed in a periglacial environment can point to which conditions, such as water availability and air and ground temperatures, were existing at the time of the feature's formation hundreds to thousands of years ago. The comparison of past conditions to the conditions of the present day can help to better understand paleoclimates and the evolution of periglacial landscapes (Lachenbruch 1962; Washburn 1980a). Periglacial geomorphology can also aid in understanding how periglacial environments will evolve in a changing global climate (Bursch 1993; Jorgenson et al. 2008; Kokelj and Jorgenson 2013; Bernard-Grand'Maison and Pollard 2018).

Studies of periglacial geomorphology have been conducted throughout many periglacial environments on Earth such as those focusing on ice-wedge development in the Lower Canadian Arctic (Mackay 1987; Mackay and Burn 2002; Morse and Burn 2013), High Canadian Arctic (Dutilleul et al. 2009; Haltigin et al. 2012; Bernard-Grand'Maison and Pollard 2018) and Antarctica (Levy et al. 2008, Mellon et al. 2014). Other periglacial features such as sorted patterned ground have been studied in Scandinavia (Uxa et al. 2017) and Antarctica (Mellon et al. 2014) to distinguish effects of climate on periglacial processes. The study of thermokarst landscapes in periglacial environments includes studies from the Low Arctic that focus on landscape evolution (Mackay 1999; Jorgenson et al. 2008) to using environments in Siberia as Mars analogues (Ulrich et al. 2011). Such studies explore periglacial features and processes that contribute to the understanding of past and current conditions of terrestrial periglacial environments, which may contribute to the study of similar environments on both Earth and Mars.

1.2 A Periglacial Mars

In recent years periglacial environments have become of particular interest to those studying the mid-latitudes of Mars (Mangold 2005, Costard et al. 2008, Lefort et al. 2009, Levy et al. 2009a, Soare et al. 2009; Séjourné et al. 2010; Haltigin et al. 2014) due to their

resemblance to terrestrial periglacial environments. Images returned from NASA's Mars Global Surveyor (MGS) mission using the Mars Orbital Camera (MOC) (Malin et al. 1992) and later by the Mars Reconnaissance Orbiter HiRISE camera (McEwen et al. 2007) revealed that the surface of Mars in the mid-latitudes displays surface patterns resembling those commonly found throughout terrestrial periglacial terrain. Specifically, smaller sized polygons (Fig. 1.2b) that appeared more similar to those found on Earth (Mangold 2005) than the kilometre-sized polygons that had been seen in images from the Mariner mission (Lucchitta 1981). The smaller polygons are considered to be thermal contraction in origin and frequently occur throughout the mid-latitudes of Mars (~30—65°) where the subsurface is proposed to be rich in ice (Mangold et al. 2004; Mangold 2005; Seibert and Kargel 2001). Polygon morphology is varied on Mars and given there is only access to remote sensing data, it is difficult to make assumptions as to what may cause morphological changes. Using Earth as an analogue for Mars may contribute to the understanding of what the diverse morphologies represent at a geologic level. The idea that Earth may represent conditions on Mars closely enough to draw conclusions about geology, hydrology and cryology has led to many investigations of terrestrial periglacial environments and their applications to Mars (e.g., Mellon 1997, Burr et al. 2009, Levy et al. 2009a, Haltigin et al. 2010; Hauber et al. 2011; Soare et al. 2011).

1.3 The Haughton Impact Structure and Devon Island

Devon Island, Nunavut (75° N, 81° W) (Fig. 1.1a) is a component of the Canadian Arctic Archipelago sitting just north of Baffin Island and covering 55, 247 km^2. The western side of the island's geology is distinguished by the Arctic Platform (Thorsteinsson and Mayr 1987) while the eastern side is largely covered in an ice cap remnant from the last glacial maximum (Dyke 1999). During the last glacial maximum, it is thought that Devon Island was mostly covered by the Innuitian Ice Sheet and was deglaciated around 8 ka (Dyke 1998, 1999). Devon Island is also home to the Haughton impact structure (75°22' N, 81°40' W) (Fig. 1.1b). The Haughton impact structure is a 23 km diameter complex impact crater that is dated at 23.5 ± 2 Ma (Young et al. 2013) and lies on the west side of Devon Island. Due to the cold, dry environment of Devon Island the Haughton impact structure is

very well preserved despite having experienced glaciation (Osinski and Lee 2005) Haughton crater itself has been studied in depth since it was first explored in the 1950's (Greiner 1963) and more so after it was confirmed as an impact structure by Robertson and Mason (1975). The target rocks at the Haughton impact structure are a thick, relatively flat lying, sedimentary sequence of predominantly carbonates of the Arctic Platform of Lower Paleozoic age (Thorsteinsson and Mayr 1987, Osinski et al. 2005a). The sedimentary succession is underlain by Precambrian metamorphic basement of the Canadian Shield (Osinski et al. 2005a). The geology within the crater is varied and includes carbonates, impactites, evaporites, a few siliciclastic rocks, post-impact lake sediments, and glacial and fluvioglacial sediments (Thorsteinsson and Mayr 1987, Osinski and Lee 2005). There are a variety of impactites throughout the crater (Fig. 1.9) that account for most of the volume of rocks as discussed in Osinski et al. (2005b) and Parnell et al. (2007). Post-impact lacustrine sediments are found in the Haughton Formation in the west of the crater and have been found to be rich in fossils of flora and fauna (Hickey et al. 1988). Glacial and fluvioglacial sediments are found throughout the crater often overlying other units (Osinski and Lee 2005). The surface outside the crater is primarily dolomite and limestone-rich Allen Bay Formation that has been eroded over time by fluvial processes and having undergone glaciation (Osinski et al. 2005a).

Devon Island is considered a polar desert as it experiences cold temperatures and very little annual precipitation. While climate data is limited, previous work has found annual precipitation to be an average of <180 mm (de Smet and Beyens 1995) in the lowlands to the east of the Haughton impact structure. The average air temperature for 2008 in the Haughton impact structure area is about -16.7 °C based on data from the Lake Orbiter weather station located ~8 km from the structure rim (Godin et al. 2018). The closest long-term climate data available is from the Resolute Bay weather station on Cornwallis Island, ~170 km west of Haughton structure, where the average air temperature is -16.4 °C and annual precipitation is ~ 150 mm (Environment Canada 2018) and is consistent with the above estimates.

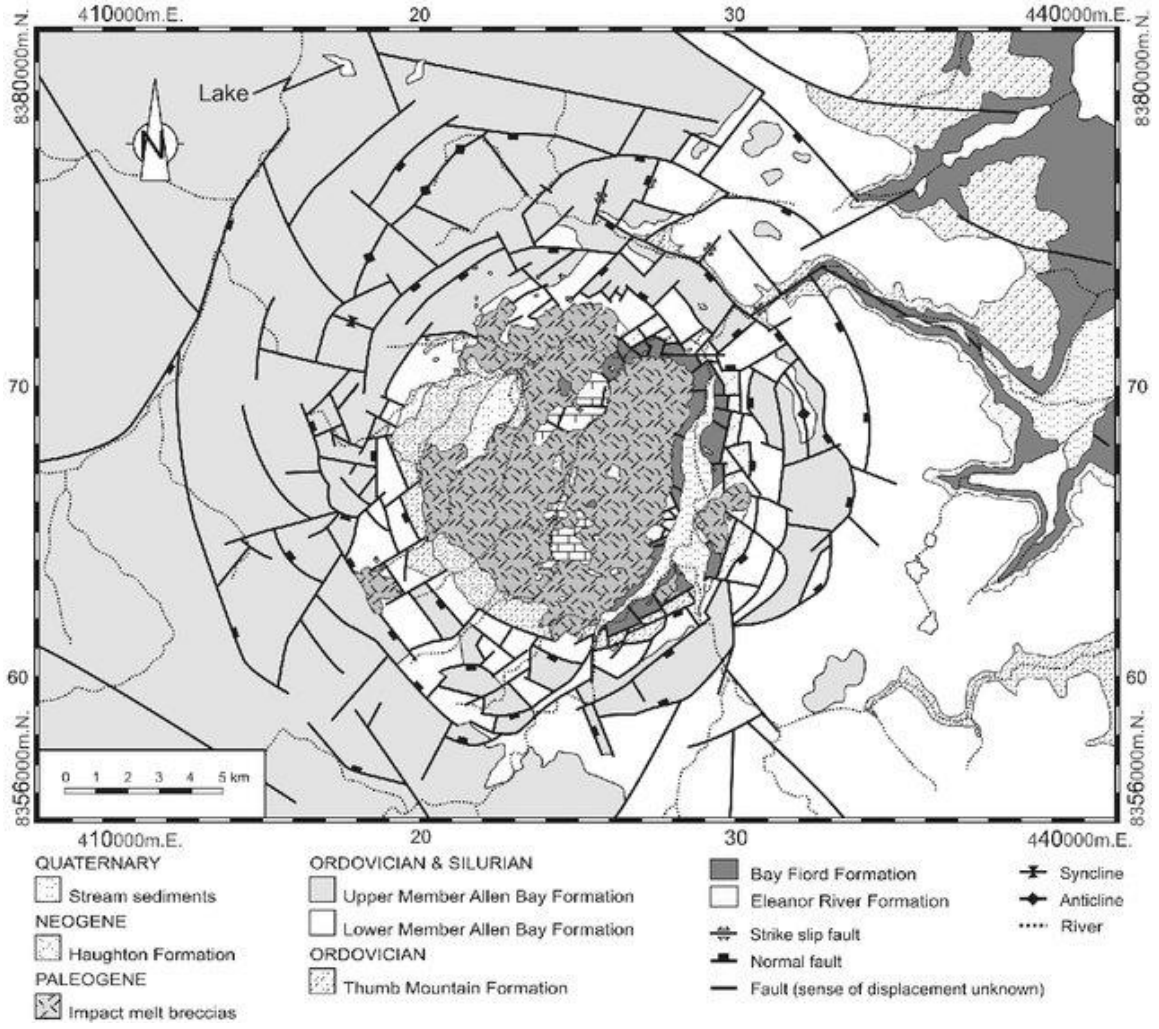

Figure 1.9: A simplified geologic map of the Haughton impact structure showing major units. From Osinski et al. 2005a.

The well-preserved impact structure along with the cold, dry environment and the presence of periglacial features makes the Haughton impact structure ideal for Mars analogue studies (Lee 1997). As such, several Mars analogue studies have taken place on Devon Island exploring geologic features (Lee 2000; Lee and Osinski 2005; Haltigin et al. 2010), technology uses (Osinski et al. 2010), astrobiology (Parnell et al. 2005; Léveillé 2009) and human response to remote scientific work (Bishop et al. 2010).

1.4 Previous Work

While studies of thermal contraction polygons have taken place readily in the low Arctic (MacKay 2000; Mackay and Burn 2002; Morse and Burn 2013; Steedman et al. 2017), Antarctica (Marchant et al. 2002; Levy et al. 2008; Mellon et al. 2014) and Scandinavia (Friedman et al. 1971; Christiansen 2005; Ulrich et al. 2011), polygon morphology in the High Arctic is not well constrained. Due to the remote and harsh nature of the High Arctic, studies of ice-wedge polygons in Arctic polar deserts, and on Devon Island specifically, are limited. Previous work on Devon Island polygons have been localized primarily in Thomas Lee Inlet located 25 km west of the Haughton impact structure (Singleton et al. 2010; Haltigin et al. 2012). Studies regarding the electromagnetic characterization of the ice-wedge polygons in Thomas Lee Inlet by Singleton et al. (2010) found that subsurface ice-wedges and massive ice could be detected using an electromagnetic induction sensor. The ice-wedge polygons in Thomas Lee Inlet have also been investigated for their development of regularity over time using spatial point pattern analysis (SPPA) by Haltigin et al. (2012). The SPPA study found that present day and historical configurations of ice-wedge polygons showed significant regularisation throughout the evolution of the polygon terrain (Haltigin et al. 2012). SPPA was also applied to ice-wedge polygons on Axel Heiberg Island (79° N, 91° W), another site of significant High Arctic polygon terrain, by Dutilleul et al. (2009) examining nearest neighbour distances and regularity, and Haltigin et al. (2010) where it was found that the most accurate characterization of ice-wedge polygon geometry came from a combination of high-resolution image analysis and ground-truthing. Other locations of High Arctic ice-wedge polygon studies include Ellesmere Island (80° N, 72° W) where work by Bernard-Grand'Maison and Pollard (2018) was conducted to estimate large-scale ice-wedge volumes, including the whole of the Fosheim Peninsula, as well as ice-wedge polygon development and historical geomorphology work on Bylot Island (73° N, 79° W) by Fortier and Allard (2004).

This thesis will report on the properties and characteristics of ice-wedge polygon terrain throughout the study area of the Haughton impact structure on Devon Island. This work aims to characterise High Arctic polygonal terrain through GIS analysis and provide insight into the factors influencing variations in ice-wedge polygon morphology. Chapter 2

reviews background information and describes the methodology used in collecting and analysing data for the study, including field measurements of polygons, troughs and the local thaw depth as well as LiDAR scanning of each site to create high-resolution DTMs. The DTMs, analyzed through GIS software, allow characterisation of High Arctic polygon geomorphology, including polygon size, shape and intersection type, at each study site. Chapter 2 will show results, including observations of unexpected variations in polygon orthogonality and inter-polygon patterned ground. Chapter 2 discusses the observations from analyses including how this study is or is not supported by previous studies of ice-wedge polygons and the implications of significant variations in polygon morphology. Chapter 3 provides conclusions and suggestions for future work on ice-wedge polygons and the areas that host them.

1.5 References

Ballantyne C.K. 2013. Patterned ground. In Encyclopedia of Quaternary Science, Second edition, Elias SA, Mock CJ (eds). Elsevier: Amsterdam, Netherlands; 452–463.

Barsch, D. 1993. Periglacial geomorphology in the 21st century. Geomorphology, **7**:141–163.

Bernard-Grand'Maison, C., and Pollard, W.H. 2018. An estimate of ice wedge volume for a High Arctic polar desert environment, Fosheim Peninsula, Ellesmere Island. The Cryosphere Discussions,: 1–28.

Bertran, P., Andrieux, E., Antoine, P., Deschodt, L., Font, M., and Sicilia, D. 2017. Pleistocene involutions and patterned ground in France: examples and analysis using a GIS database. Permafrost and Periglacial Processes, **28**: 710–725.

Bishop, S.L., Kobrick, R., Battler, M., and Binsted, K. 2010. FMARS 2007: Stress and coping in an arctic Mars simulation. Acta Astronautica, **66**: 1353–1367.

Black, R.F. 1976. Periglacial features indicative of permafrost: Ice and soil wedges. Quaternary Research, **6**: 3–26.

Burr, D.M., Tanaka, K.L., and Yoshikawa, K. 2009. Pingos on Earth and Mars. Planetary and Space Science, **57**: 541–555.

Christiansen, H.H. 2005. Thermal regime of ice-wedge cracking in Adventdalen, Svalbard.

Permafrost and Periglacial Processes, **16**: 87–98.

Costard, F., Forget, F., Madeleine, J.B., Soare, R.J., and Kargel, J. 2008. The origin and formation of scalloped terrain in Utopia Planitia: Insight from a general circulation model. Lunar and Planetary Science Conference, **39th**: 1274 pdf.

de Smet, W.H., Beyens, L. 1995. Rotifers from the Canadian High Arctic (Devon Island, Northwest Territories). Hydrobiologia 313/314: 29–34.Dobiński, W. 2011. Permafrost. Earth-Science Reviews, **108**: 158–169.

Dutilleul, P., Haltigin, T.W., and Pollard, W.H. 2009. Analysis of polygonal terrain landforms on Earth and Mars through spatial point patterns. Environmetrics, **20**: 206–220.

Dyke, A.S. 1998. Holocene delevelling of Devon Island, Arctic Canada: implications for ice sheet geometry and crustal response. Canadian Journal of Earth Sciences, **35**: 885–904.

Dyke, A.S. 1999. Last Glacial Maximum and deglaciation of Devon Island, Arctic Canada: Support for an Innuitian ice sheet. Quaternary Science Reviews, **18**: 393–420.

Environment Canada. Canadian climate normals, 1961–1990. Resolute. 2018. http://climat.meteo.gc.ca/climate_normals/.

Feuillet, T., Mercier, D., Decaulne, A., and Cossart, E. 2012. Geomorphology Classi fication of sorted patterned ground areas based on their environmental characteristics (Skagafjörður , Northern Iceland). Geomorphology, **139**–**140**: 577–587.

Fortier, D., and Allard, M. 2004. Late Holocene syngenetic ice-wedge polygons development, Bylot Island, Canadian Arctic Archipelago. Canadian Journal of Earth Sciences, **41**: 997–1012.

Fortier, D., and Allard, M. 2005. Frost-cracking conditions, Bylot Island, eastern Canadian Arctic archipelago. Permafrost and Periglacial Processes, **16**: 145–161.

French, H.M. 2000. Does Lozinski's periglacial realm exist today? A discussion relevant to modern usage of the term "periglacial." Permafrost and Periglacial Processes, **11**: 35–42.

French, H.M. 2007. The Periglacial Environment. 3rd ed. John Wiley, Chichester, UK

Friedman, J.D., Johansson, C.E., Oskarsson, N., Svensson, H., Thorarinsson, S., and Williams, R.S. 1971. Observations on Icelandic polygon surfaces and palsa areas.

Photo Interpretation and Field Studies. Geografiska Annaler. Series A, Physical Geography, **53**: 115–145. [Wiley, Swedish Society for Anthropology and Geography].

Godin, E., Osinski, G. R., Harrison, T. Zanetti, M. 2018. Geomorphology of gullies at Thomas Lee Inlet, Devon Island, Canadian High Arctic. Permafrost and Periglacial Processes. (accepted)

Haltigin, T.W., Pollard, W.H., and Dutilleul, P. 2010. Comparison of ground- and aerial-based approaches for quantifying polygonal terrain network geometry on Earth and Mars via spatial point pattern analysis. Planetary and Space Science, **58**: 1636–1649. Elsevier.

Haltigin, T.W., Pollard, W.H., Dutilleul, P., and Osinski, G.R. 2012. Geometric evolution of polygonal terrain networks in the Canadian High Arctic: evidence of increasing regularity over time. Permafrost and Periglacial Processes, **23**: 178–186.

Haltigin, T.W., Pollard, W.H., Dutilleul, P., Osinski, G.R., and Koponen, L. 2014. Co-evolution of polygonal and scalloped terrains, southwestern Utopia Planitia, Mars. Earth and Planetary Science Letters, **387**: 44–54.

Hauber, E., Reiss, D., Ulrich, M., Preusker, F., Trauthan, F., Zanetti, M., Hiesinger, H., Jaumann, R., Johansson, L., Johnsson, A., Van Gasselt, S., and Olvmo, M. 2011. Landscape evolution in Martian mid-latitude regions: insights from analogous periglacial landforms in Svalbard. Geological Society, London, Special Publications, **356**: 111 LP-131. Available from http://sp.lyellcollection.org/content/356/1/111.abstract. [accessed on 15 June 2018].

Hickey, L.J., Johnson, K.R., and Dawson, M.R. 1988. The stratigraphy, sedimentology, and fossils of the Haughton formation: A post-impact crater-fill. Meteoritics, **23**: 221–231.

Jorgenson, M.T., and Osterkamp, T.E. 2005. Response of boreal ecosystems to varying modes of permafrost degradation 1. Canadian Journal for Res., **35**: 2100–2111.

Jorgenson, M.T., Shur, Y.L., and Osterkamp, T.E. 2008. Thermokarst in Alaska. Ninth International Conference on Permafrost. 2008. doi:10.1017/CBO9781107415324.004.

Klene, A.E., Nelson, F.E., Shiklomanov, N.I., and Hinkel, K.M. 2001. The N-Factor in

Natural Landscapes: Variability of air and soil-surface temperatures, Kuparuk River Basin, Alaska, U.S.A. Arctic, Antarctic, and alpine research, **33**: 140–148.

Kokelj, S. V., and Jorgenson, M.T. 2013. Advances in thermokarst research. Permafrost and Periglacial Processes, **24**: 108–119.

Lachenbruch, A.H. 1962. Mechanics of Thermal Contraction Cracks and Ice-Wedge Polygons in Permafrost. Geologic Society of America Special Papers, **70**.

Lee, P., and Osinski, G.R. 2005. The Haughton-Mars Project: Overview of science investigations at the Haughton impact structure and surrounding terrains, and relevance to planetary studies. Meteoritics and Planetary Science, **40**: 1777–1787.

Lefort, A., Russell, P.S., Thomas, N., McEwen, A.S., Dundas, C.M., and Kirk Physikalisches, R.L. 2009. Observations of periglacial landforms in utopia planitia with the high resolution imaging science experiment (HiRISE). Journal of Geophysical Research E: Planets, **114**: 1–18.

Léveillé, R. 2009. Validation of astrobiology technologies and instrument operations in terrestrial analogue environments. Comptes Rendus - Palevol, **8**: 637–648.

Levy, J.S., Head, J.W., and Marchant, D.R. 2008. The role of thermal contraction crack polygons in cold-desert fluvial systems. Antarctic Science, **20**: 565–579.

Levy, J.S., Head, J.W., and Marchant, D.R. 2009a. Thermal contraction crack polygons on Mars: Classification, distribution, and climate implications from HiRISE observations. Journal of Geophysical Research E: Planets, **114**: 1–19.

Levy, J.S., Head, J.W., Marchant, D.R., Dickson, J.L., and Morgan, G.A. 2009b. Geologically recent gully-polygon relationships on Mars: Insights from the Antarctic Dry Valleys on the roles of permafrost, microclimates, and water sources for surface flow. Icarus, **201**: 113–126.

Lucchitta, B.K. 1981. Mars and Earth: Comparison of cold-climate features. Icarus, **45**: 264–303.

Mackay, J.R. 1962. Origin of the pingos of the pleistocene Mackenzie Delta area (Summary). In Proceedings of the First Canadian Conference on Permafrost. Ottawa, ON. 79–83.

Mackay, J.R. 1972. The World of Underground Ice. Arctic, **62**: 1–22.

Mackay, J.R. 1979. Pingos of the Tuktoyaktuk Peninsula Area, Northwest Territories.

Géographie physique et Quaternaire, **33**: 3–61.

Mackay, J.R. 1980. Deformation of ice-wedge polygons, Garry Island, Northwest Territories. *In* Geological Survey of Canada Paper. 80–1A. 287–291.

Mackay, J.R. 1987. Some mechanical aspects of pingo growth and failure, western Arctic coast, Canada. Canadian Journal of Earth Sciences, **24**: 1108–1119.

Mackay, J.R. 1990. Some observations on the growth and deformation of epigenetic, syngenetic and anti-syngenetic ice wedges. Permafrost and Periglacial Processes, **1**: 15–29.

Mackay, J.R. 1993. Air temperature, snow cover, creep of frozen ground, and the time of ice-wedge cracking , western Arctic coast. Canadian Journal of Earth Sciences, **30**: 1720–1729.

Mackay, J.R. 1999. Periglacial features developed on the exposed lake bottoms of seven lakes that drained rapidly after 1950, Tuktoyaktuk Peninsula area, western Arctic coast, Canada. Permafrost and Periglacial Processes, **10**: 39–63.

Mackay, J.R. 2000. Thermally induced movements in ice-wedge polygons, western arctic coast: a long-term study. Géographie physique et Quaternaire, **54**: 41–68.

Mackay, J.R., and Burn, C.R. 2002. The first 20 years (1978-1979 to 1998-1999) of ice-wedge growth at the Illisarvik experimental drained lake site, western Arctic coast, Canada. Canadian Journal of Earth Sciences, **39**: 95–111.

Malin, M.C., Danielson, G.E., Ingersoll, A.P., Masursky, H., Veverka, J., Ravine, M.A., and Soulanille, T.A. 1992. Mars Observer Camera. Journal of Geophysical Research, **97**: 7699-7718

Mangold, N. 2005. High latitude patterned grounds on Mars: Classification, distribution and climatic control. Icarus, **174**: 336–359.

Mangold, N., Maurice, S., Feldman, W.C., Costard, F., and Forget, F. 2004. Spatial relationships between patterned ground and ground ice detected by the Neutron Spectrometer on Mars. Journal of Geophysical Research E: Planets, **109**: 1–6.

Marchant, D.R., Lewis, A.R., Phillips, W.M., Moore, E.J., Souchez, R.A., Denton, G.H., Sugden, D.E., Potter N., J., and Landis, G.P. 2002. Formation of patterned ground and sublimation till over Miocene glacier ice in Beacon Valley, southern Victoria Land, Antarctica. GSA Bulletin, **114**: 718–730.

McEwen, A.S., Eliason, E.M., Bergstrom, J.W., Bridges, N.T., Hansen, C.J., Delamere, W.A., Grant, J.A., Gulick, V.C., Herkenhoff, K.E., Keszthelyi, L., Kirk, R.L., Mellon, M.T., Squyres, S.W., Thomas, N., and Weitz, C.M. 2007. Mars Reconnaissance Orbiter's High Resolution Imaging Science Experiment (HiRISE). Journal of Geophysical Research: Planets, **112**: 1–40.

Mellon, M.T. 1997. Small-scale polygonal features on Mars: Seasonal thermal contraction cracks in permafrost. Journal of Geophysical Research: Planets, **102**: 25617–25628.

Mellon, M.T., McKay, C.P., and Heldmann, J.L. 2014. Polygonal ground in the McMurdo Dry Valleys of Antarctica and its relationship to ice-table depth and the recent Antarctic climate history. Antarctic Science, **26**: 413–426.

Morse, P.D., and Burn, C.R. 2013. Field observations of syngenetic ice wedge polygons, outer Mackenzie Delta, western Arctic coast, Canada. Journal of Geophysical Research: Earth Surface, **118**: 1320–1332.

Müller, F. 1959. Observations on pingos. NRC Publications Archive, **153:** 5–117.

Osinski, G.R., Barfoot, T.D., Ghafoor, N., Izawa, M., Banerjee, N., Jasiobedzki, P., Tripp, J., Richards, R., Auclair, S., Sapers, H., Thomson, L., and Flemming, R. 2010. Lidar and the mobile Scene Modeler (mSM) as scientific tools for planetary exploration. Planetary and Space Science, **58**: 691–700.

Osinski, G.R., and Lee, P. 2005. Intra-crater sedimentary deposits at the Haughton impact structure, Devon Island, Canadian High Arctic. Meteoritics & Planetary Science, **40**: 1887–1899.

Osinski, G.R., Lee, P., Spray, J.G., Parnell, J., Lim, D., Bunch, T.E., Cockell, C.S., and Glass, B. 2005a. Geological overview and cratering model for the Haughton impact structure, Devon Island, Canadian High Arctic. Meteoritics and Planetary Science, **40**: 1759–1776.

Osinski, G.R., Spray, J.G., and Lee, P. 2005b. Impactites of the Haughton impact structure, Devon Island, Canadian High Arctic. Meteoritics and Planetary Science, **40**: 1789–1812.

Parnell, J., Bowden, S.A., Osinski, G.R., Lee, P., Green, P., Taylor, C., and Baron, M. 2007. Organic geochemistry of impactites from the Haughton impact structure, Devon Island, Nunavut, Canada. Geochimica et Cosmochimica Acta, **71**: 1800–1819.

Parnell, J., Lee, P., Osinski, G.R., and Cockell, C.S. 2005. Application of organic geochemistry to detect signatures of organic matter in the Haughton impact structure. Meteoritics and Planetary Science, **40**: 1879–1885.

Pletser, V., Lognonne, P., Diament, M., and Dehant, V. 2009. Subsurface water detection on Mars by astronauts using a seismic refraction method: Tests during a manned Mars simulation. Acta Astronautica, **64**: 654–655.

Seibert, N.M., and Kargel, J.S. 2001. Small scale martain polygonal terrain: Implications for liquid surface water. Geophysical Research letters, **28**: 899–902.

Séjourné, A., Costard, F., Gargani, J., Soare, R.J., and Marmo, C. 2010. Polygon junction pits as evidence of a particularly ice-rich area in Utopia Planitia, Mars. Lunar and Planetary Science Conference, **41**: 2113.

Singleton, A.C., Osinski, G.R., Samson, C., Williamson, M.C., and Holladay, S. 2010. Electromagnetic characterization of polar ice-wedge polygons: Implications for periglacial studies on Mars and Earth. Planetary and Space Science, **58**: 472–481.

Soare, R.J., and Osinski, G.R. 2009. Stratigraphical evidence of late Amazonian periglaciation and glaciation in the Astapus Colles region of Mars. Icarus, **202**: 17–21.

Soare, R.J., Séjourné, A., Pearce, G., Costard, F., and Osinski, G.R. 2011. The Tuktoyaktuk Coastlands of northern Canada: A possible “wet” periglacial analog of Utopia Planitia, Mars. *In* Special Paper of the Geological Society of America.

Steedman, A.E., Lantz, T.C., and Kokelj, S. V. 2017. Spatio-temporal variation in high-centre polygons and ice-wedge melt ponds, Tuktoyaktuk Coastlands, Northwest Territories. Permafrost and Periglacial Processes, **28**: 66–78.

Thorsteinsson, R., and Mayr, U. 1987. The sedimentary rocks of Devon Island, Canadian Arctic Archipelago. Geological Survey of Canada Memoir, **411**: 1–182.

Treml, V., Krizek, M., and Engel, Z. 2010. Classification of patterned ground based on morphometry and site characteristics: A case study from the High Sudetes, central Europe. Permafrost and Periglacial Processes, **21**: 67–77.

Ulrich, M., Hauber, E., Herzschuh, U., Härtel, S., and Schirrmeister, L. 2011. Polygon pattern geomorphometry on Svalbard (Norway) and western Utopia Planitia (Mars) using high-resolution stereo remote-sensing data. Geomorphology, **134**: 197–216.

Uxa, T., Mida, P., and Křížek, M. 2017. Effect of climate on morphology and development of sorted circles and polygons. Permafrost and Periglacial Processes, **28**: 663–674.

van Everdingen, R.O. 1998. Multi-language glossary of permafrost and related ground-ice terms. Arctic and Alpine Research, **21**: 213. doi:10.2307/1551636.

Washburn, A.L. 1956. Classification of patterned ground and review of suggested origins. Bulletin of the Geological Society of America. **67**. 823–866

Washburn, A.L. 1980a. Geocryology. A survey of periglacial processes and environments. The Blackburn Press, New Jersey.

Washburn, A.L. 1980b. Permafrost features as evidence of climatic change. Earth Science Reviews, **15**: 327–402.

Young, K.E., Van Soest, M.C., Hodges, K. V., Watson, E.B., Adams, B.A., and Lee, P. 2013. Impact thermochronology and the age of Haughton impact structure, Canada. Geophysical Research Letters, **40**: 3836–3840.

Zhang, T., Barry, R.G., Knowles, K., Heginbottom, J.A., and Brown, J. 1999. Statistics and characteristics of permafrost and ground-ice distribution in the northern hemisphere. Polar Geography, **23**: 132–154.

Chapter 2

2 Characterizing Ice-wedge Polygon Geomorphology in the Haughton Impact Structure, Devon Island

Periglacial environments are dominated by non-glacial, cold processes and display a wide range of landforms formed due to cyclical freezing and thawing processes. Polygon terrain is a distinctive and widespread periglacial landform found in most unconsolidated sediments throughout areas of permafrost in high latitudes and altitudes (e.g., French 2007). Polygon formation and networks within some permafrost environments such as Svalbard, Norway (Ulrich et al. 2011) Antarctica (Mellon et al. 2014) and the Canadian Arctic (Mackay 1972, 1999, 2000) have been described in detail in the literature (Lachenbruch 1962; Washburn 1980; French 2007). Thermal contraction polygons are characterized by thermal contraction cracks that occur in the frozen ground upon intense cooling over a short time interval (Fortier and Allard 2005). Extensive networks of contraction cracks occur across areas of permafrost to form networks of polygon terrain. Polygons with ice-filled cracks are known as ice-wedge polygons and are indicative of thermal fluctuations, permafrost and liquid water presence at the surface (Washburn 1980). In more arid environments other materials may enter the cracks and form sand- or debris-wedge polygons (Black 1976; Mellon et al. 2014). The distinction of conditions that allow for the formation of ice-wedge polygons is well documented (Lachenbruch 1962; Washburn 1980; Mackay 1993; Mackay and Burn 2002); however, the driving forces for variation in polygon surface morphology in Arctic environments is not as well constrained. The environmental conditions present on Devon Island in the Canadian High Arctic (Fig. 2.1a) are that of a polar desert (e.g., Osinski et al. 2005) and the polygons in and around the Haughton impact structure (Fig. 2.1b) are varied in their morphology despite being subject to the same ubiquitous cold, arid conditions. The Haughton impact structure may offer insight into the factors influencing the differences in polygon morphology in a relatively small area experiencing the same polar desert climate.

2.1 Thermal Contraction Polygons

Ice-wedge polygons form in permafrost through thermal contraction cracking in winter. In spring when thaw occurs the open cracks are filled with water which freezes at depth within the permafrost forming a vein of ice (Lachenbruch 1962; Mackay 1990). The vein and ground freeze entirely in winter at which point the ground may re-crack again upon intense cooling (Lachenbruch 1962). The cycle of water in-filling in spring and contraction cracking in winter repeats for tens to hundreds of years causing the ice-filled cracks to become wedge-shaped ice bodies (Lachenbruch 1962; Mackay 1993; Fortier and Allard 2005). With the right conditions ice wedges can continue to grow and become very thick; however, once the tensile strength of an ice-wedge becomes more than the stresses of the frozen ground, growth will stop, and the ice-wedge will remain mostly stable in size until conditions change (Lachenbruch 1962). The growth of an ice-wedge pushes material from the edges towards the centre of the polygon as the growing wedge displaces sediment (Mackay 2000; French 2007). There also exists a lateral temperature driven movement of sediments from the centre of the polygon to the sides within the thawed active layer during the summer months (Mackay 1980; 2000; French 2007). The combination of these two factors creates a raised rim along the ice-wedge crack making the polygon centre appear lower relative to the raised rim. This morphology is known as a low-centred polygon ("lcp"). When ice-wedges around a lcp begin to degrade due to thermal instability, they leave behind sunken troughs and the polygon centres may consequently appear raised above the contouring trough. Polygons with this morphology are known as high-centred polygons ("hcp") (Washburn 1980; Mackay 2000). The distinct differences in the morphology of hcp and lcp are thought to reflect a change in environmental or climatic conditions (Lachenbruch 1962; Mackay 2000; Jorgenson et al. 2006; Mellon et al. 2014; Abolt et al. 2017). Changes in air and/or ground temperature, surface energy budget, water availability, water pooling, vegetation cover and erosion rates will all ultimately change the morphology of polygons (Washburn 1980, Mackay 1990; Mackay and Burn 2002; French 2007). For example, an increase in air and/or ground temperature may result in degradation of permafrost and thickening of the active layer eventually causing unstable ice-wedges around lcps to degrade form hcps (Mackay 2000; Jorgenson and Osterkamp 2005; Jorgenson et al. 2006). This research aims to describe the internal and external

drivers behind the morphological variations observed in High Arctic ice-wedge polygons within a relatively small study area where conditions would be expected to be similar.

Given that both hcp and lcp are observed within the study area, does this indicate a significant difference in conditions within the area in and around the Haughton impact structure? This work seeks to provide further insight into this question by using both field and remote sensing methods to describe the geology and geomorphology present in the polygon terrain and report on differences in conditions observed within each study site. High-resolution DTMs were created from LiDAR scans preformed at each site to analyse the ice-wedge polygon geomorphology including size, shape and intersection type. Measurements of polygon centres and troughs as well as excavation of soil pits were completed in the field to compliment the remote sensing data and include substrate and homogeneity as factors influencing geomorphology. The main objective of this study is to determine the factors that contribute to polygon morphology in different sites within the polar desert environment of Devon Island and ultimately, to use this information to compare ice-wedge polygon morphology with similar features on Mars.

Previous studies of ice-wedge polygons have taken place in the Low Arctic (Mackay 2000; Morse and Burn 2013; Abolt et al. 2017), Scandinavia (Friedman et al. 1971; Christiansen 2005; Ulrich et al. 2011) and Antarctica (Marchant et al. 2002; Levy et al. 2009b; Mellon et al. 2014) among others. Ice-wedge polygon morphology is not well constrained in High Arctic polar desert environments. Previous work on polygons on Devon Island has occurred almost exclusively in Thomas Lee Inlet located 25 km west of the Haughton impact structure (Singleton et al. 2010; Haltigin et al. 2012). A study by Singleton et al. (2010) found that electromagnetic induction was useful in detecting subsurface ice-wedges and massive ice in Thomas Lee Inlet. Haltigin et al. (2012) used spatial point pattern analysis (SPPA) to investigate polygon regularity in Thomas Lee Inlet and found that ice-wedge polygons experienced significant regularity increases over time. Other High Arctic sites that have been the subject of study include Axel Heiberg Island (79° N, 91° W) where SPPA was used to determine accurate characterization of ice-wedge polygon geometry by Dutilleul et al. (2009) and Halitigin et al. (2010). Work on Ellesmere Island (80° N, 72° W) conducted by Bernard-Grand'Maison and Pollard (2018) was done to estimate large-

scale ice-wedge volumes across a large area including the whole of the Fosheim Peninsula. On Bylot Island (73° N, 79° W), studies on ice-wedge polygon development and historical geomorphology conducted by Fortier and Allard (2004) found that changes in the composition of the surface, such as accumulation of silt and organic sediments and increase in pore-ice, over time is more likely responsible for secondary cracking in polygon networks than climatic changes.

2.2 Periglacial Mars

In recent years periglacial environments on Earth have become of interest to those studying the mid-latitudes of Mars where a host of similar landforms have been observed (e.g., Costard et al. 2008; Haltigin et al. 2014; Lefort 2009; Levy et al. 2009; Mangold 2005; Sejourne et al. 2010; Soare et al. 2009). Specifically, smaller sized polygons that appear morphologically similar to those found on Earth are widespread (Mellon 1997, 2005). The smaller polygons are considered to be thermal contraction in origin and frequently occur throughout the mid-latitudes of Mars (~30–65°) where the subsurface is thought to be rich in ice (Mangold et al. 2004; Mangold 2005; Seibert and Kargel 2001). Polygon morphology, such as size and low/high centredness, is varied on Mars and given limited remote sensing data it is difficult to make assumptions as to what may cause morphological changes. Using Earth as an analogue for Mars may contribute to the understanding of what the varying morphologies represent at a geologic level. The notion that some places on Earth may represent conditions on Mars closely enough to draw conclusions about geology, hydrology and cryology has led to many investigations of terrestrial periglacial environments and their applications to Mars (e.g., Levy et al. 2009a; Haltigin et al. 2010; Hauber et al. 2011; Ulrich et al. 2011). This study aims to contribute to analogue studies of Earth and Mars to provide further evidence of how polygon networks reflect certain conditions.

2.3 Geology of the Study Sites

2.3.1 Devon Island and the Haughton Impact Structure

Devon Island is the largest uninhabited island in the Arctic Archipelago in the Canadian High Arctic and is host to the Haughton impact structure (75°22’ N, 81°40’ W) (Fig. 2.1a). The Haughton impact structure (Fig. 2.1b) is a well-preserved complex meteorite impact crater formed 23.5 ± 2 million years ago (Young et al. 2013). The 23 km wide structure formed in sedimentary rocks of the Arctic Platform overlying the Precambrian Shield.

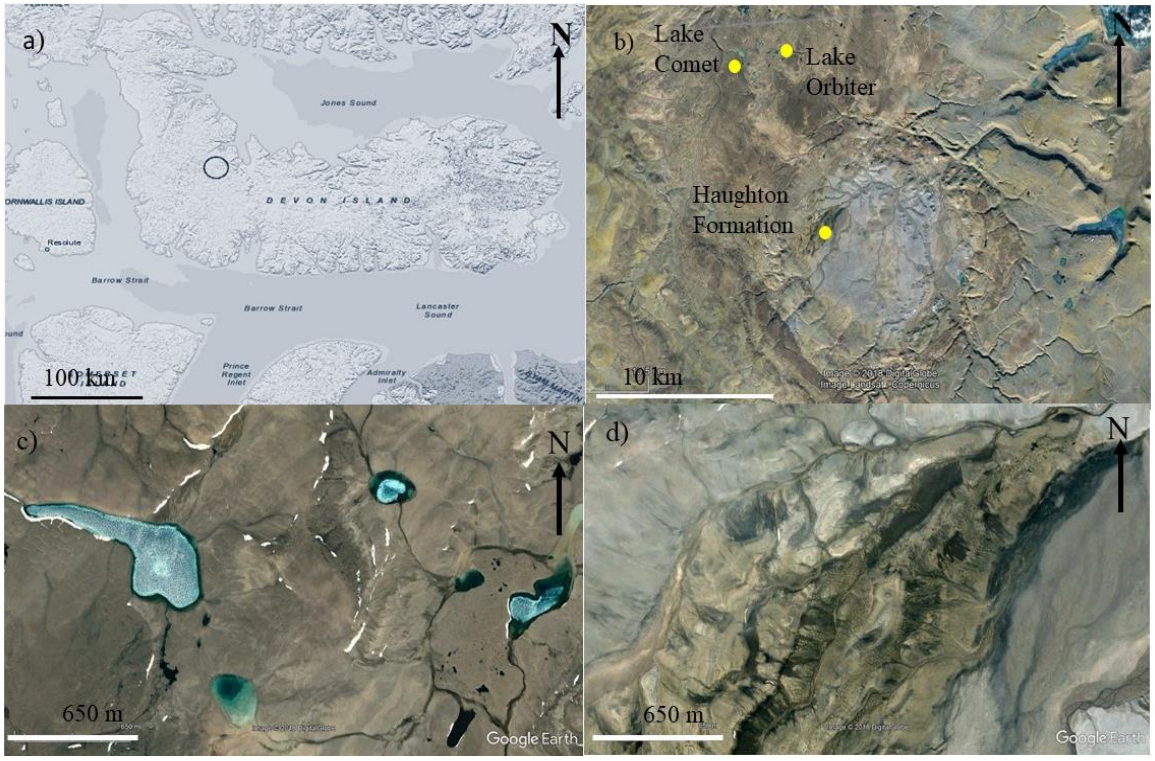

Figure 2.1: a) Devon Island, Nunavut with a circle indicating the location of the Haughton impact structure. b) A 2018 DigitalGlobe / Landsat / Copernicus image of the Haughton impact structure showing the three field site locations (Google Earth 2018). c) A 2018 DigitalGlobe image of the Lake Comet (left) and Lake Orbiter (right) field sites. d) A 2018 DigitalGlobe image of the Haughton Formation field site.

The rocks around the crater are a relatively flat, dolomite limestone unit known as the Allen Bay Formation that is dated as Upper Ordovician (Thorsteinsson and Mayr 1987; Osinski

et al. 2005). The geology within the crater itself is varied and includes carbonates, impactites, post-impact lake sediments, and glacial and fluvioglacial sediments (Osinski et al. 2005a). There are a variety of impactites throughout the crater that are discussed in Osinski et al. (2005b) and Parnell et al. (2007). Post-impact Miocene-aged lacustrine sediments of the Haughton Formation are present in the west of the crater and have been found to be rich in fossils of flora and fauna (Hickey et al. 1988; Osinski and Lee 2005). Glacial and fluvioglacial sediments are found throughout the crater often overlying other units (Osinski and Lee 2005). The three sites discussed in this study cover a range of geologic and topographic locations that are present in and around the Haughton impact structure (Fig. 2.1b) which is considered an excellent analogue to Mars (Lee and Osinski 2005)

The east side of Devon Island is host to an ice cap remnant from the last glacial maximum when it is thought that Devon Island was covered by the Innuitian Ice Sheet (Dyke 1998). The island deglaciated around eight thousand years ago, making way for periglacial processes to dominate the landscape (Dyke 1999). Devon Island is considered a polar desert as it experiences very little annual precipitation with an average of <180 mm in the True Love Lowlands 160 km to the east of the Haughton impact structure (de Smet and Beyens 1995). The average annual air temperature around the Haughton impact structure is about -16.7 °C based on data from a weather station at Lake Orbiter (Godin et al. 2018). The closest permanent weather station is found in Resolute, approximately 170 km east of the Haughton impact structure, where annual precipitation is ~150 mm and the average annual air temperature -16.4 °C (Environment Canada 2018).

2.3.2 Study Sites

The Haughton Formation

The Haughton Formation (75° 23’N 89° 48’W) covers ~8 km^2 located in the western part of the Haughton impact structure (Fig. 2.1b). The large formation is 130–140 m above sea level (a.s.l.) and consists of fine-grained dolomite-rich lacustrine sediments deposited within the structure post-impact (Hickey et al. 1988). The paleolacustrine unit has been measured to be ~48 m thick overlying both lower Paleozoic target rocks and impact melt

rocks (Hickey et al. 1988; Osinski and Lee 2005). The formation is relatively low lying with hills and terraces throughout. It is one of the few places in the surrounding landscape that has partial vegetation cover of grasses and moss (Figs. 2.2a, b, c). The unit features areas of pooling water and seasonal streams that run through the boundaries of the lowest lying areas (Fig. 2.2d).

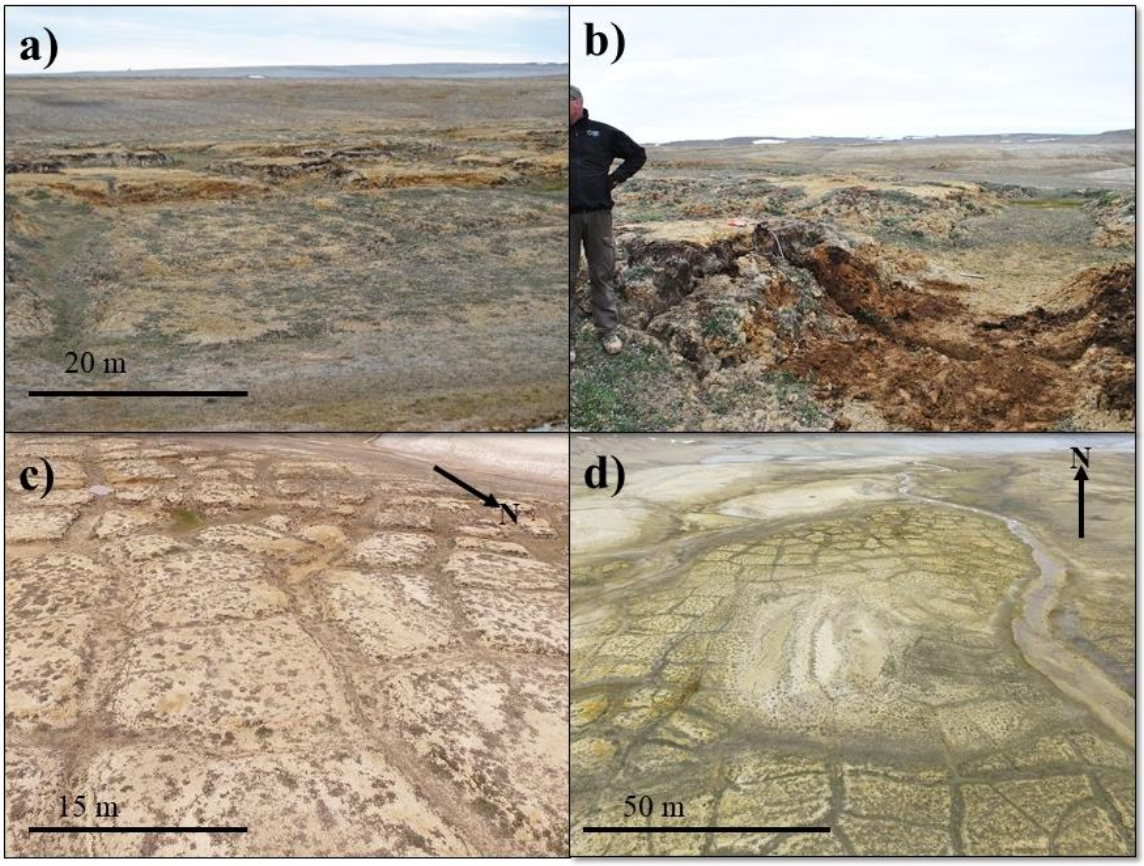

Figure 2.2: a) Ground image of high-centred polygons within the Haughton Formation. b) Ground image showing the degraded edges of hcp and the site of a trench dug through the active layer. c & d) Aerial drone views of the Haughton Formation. (July 2017)

Lake Comet

Lake Comet is an elongated east–west, 0.25 km^2 lake (75° 29'N 89° 58'W) located at 195 m a.s.l, ~7 km beyond the rim of the northern side of the Haughton impact structure (Fig.

2.1b). The surface of the site is covered by a felsenmeer of Allen Bay Formation dolomites. The block size varies from centimetre to decimetre in size (Fig. 2.3a, b, c). The lake is surrounded on almost all sides by rounded hills (Fig. 2.3b), with the exception of the south-east corner of the lake where there is a flat riverbed. The environment at Lake Comet at the time of observation was wet from both meltwater and rain. In late July ice remained on the lake in addition to snow along the shore, on nearby hillsides and within some polygon troughs (Fig. 2.3b, d).

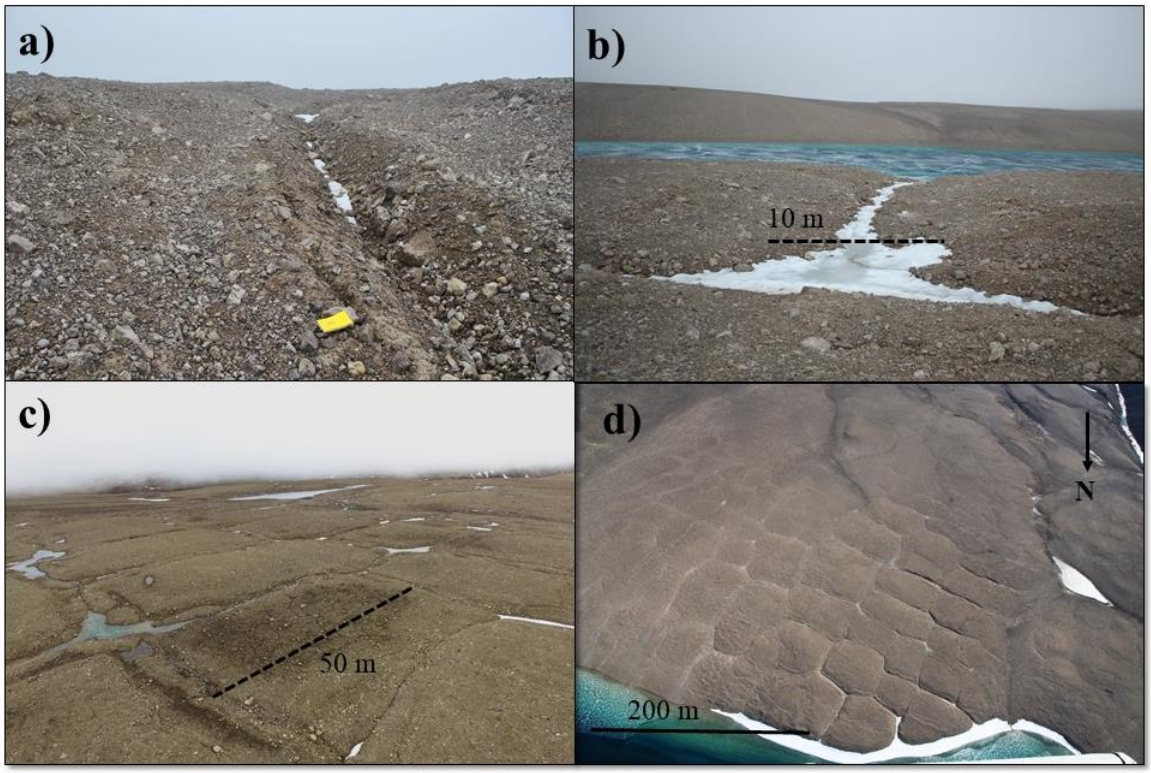

Figure 2.3: a) Trough of a large hcp at Lake Comet. b) A snow-filled three-ray trough intersection next to raised polygon centres c) Drone image (20 m) view of Lake Comet hcp. d) Helicopter image of Lake Comet site, polygons are ~50 m across. (a–c July 2017, d: 2007)

Lake Orbiter

The Lake Orbiter study site (75° 29'N 89° 52'W) is a flat plain host to low relief periglacial landforms such as patterned ground (Fig. 2.4a), with a 0.12 km^2 lake along the eastern side of the plain. The site is located to the northeast of the Haughton impact structure at 180 m a.s.l., ~7 km outside the rim and 2.5 km east of Lake Comet (Fig. 2.1b). The Lake Orbiter site consists of small to medium, centimetre-sized sub-rounded to sub-angular cobbles of fluvioglacial sediments that are derived from the Allen Bay Formation (Fig. 2. 4b, c). Small streams are surrounding the plain to the north, west and south as well as areas of slight hills and higher topography to the north, west and east beyond the streams (Fig. 2.4d). Neither gullies nor large snow patches were observed on the surrounding hills; however, much of the lake was still frozen and there were small snow patches and ice remaining on hill slopes and along the shore of the lake. Water appeared to be draining toward the lake from several sources, including through some polygon troughs and from the largest stream feeding the lake from the south (Fig. 2.4d).

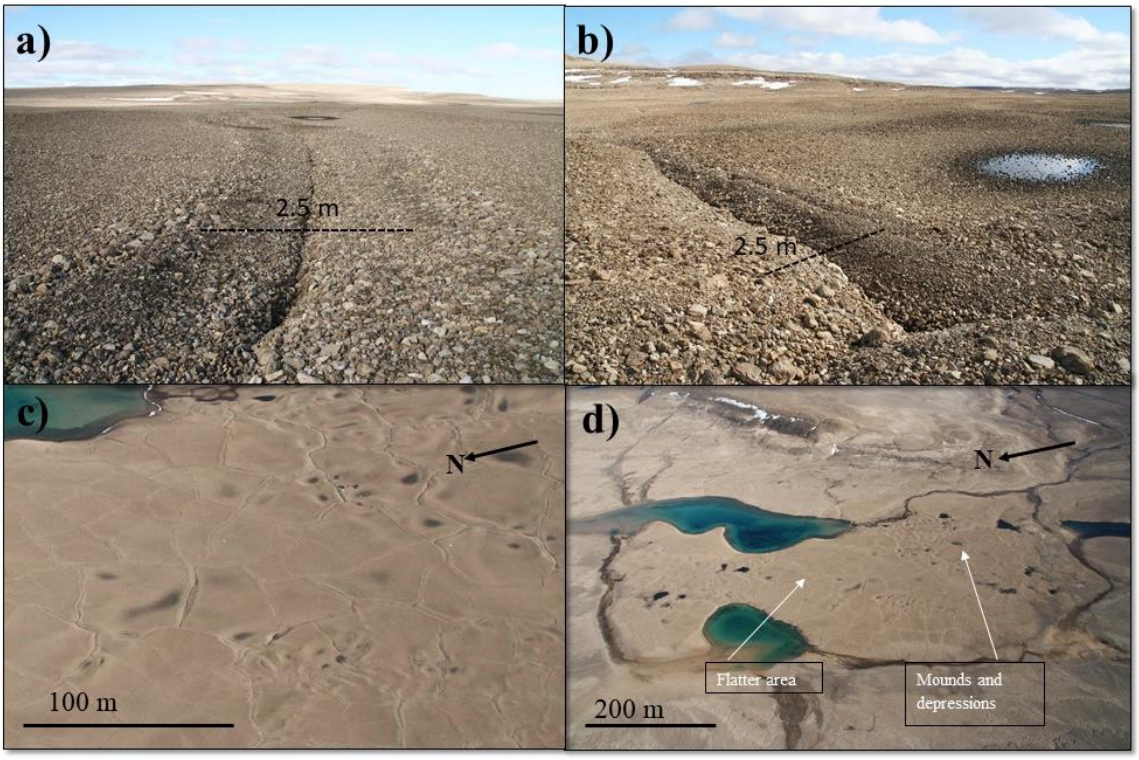

Figure 2.4: a) Aerial view of Lake Orbiter lcp showing more orthogonal polygons on the left of the image and non-orthogonal on the right. b) A three-ray trough intersection next to a depressed polygon centre with pooling water c) Trough of a large lcp at Lake Orbiter. d) Airborne oblique photo of Lake Orbiter site, arrow highlighting flatter northern area and southern area with mounds and depressions. (a and d: 2007, b and c: 2017)

2.4 Data Collection and Methods

Detailed investigation of three sites on Devon Island that display thermal contraction polygon networks took place in July 2017. Each site, described above, contains 25 or more continuous polygons within two geologic units. WorldView satellite imagery from 2013, ground imagery from 2007 to 2016, and LiDAR data were also used to locate and map potential field targets. At each site, a polygon with well-formed troughs and that was fully enclosed by other polygons was chosen at random for a soil pit and sampling. A soil pit was dug in the sample polygon centre and trough, to the maximum extent of the thaw depth. The soil pits allowed for the observation and interpretation of the shallow subsurface

stratigraphy as well as the thaw depth. In the Haughton Formation site, a trench was dug across a trough from one edge of the sample polygon, through the trough, to the edge of a neighbouring polygon. The trench was 5.5 m across along the bottom (Fig. 2.2b). A trench was dug only at the Haughton Formation site because the fine grain substrate allowed for such extensive digging down to the extent of the thaw depth. The trench was used to observe potential ice-wedge thickness and changes in stratigraphy from the polygon centre to the trough. To build on the subsurface data from the soil pits, a steel probe was used to measure the thaw depth above the permafrost at each site. In fine-grained substrates, two 20 m long transects intersecting in a polygon centre at 90º were laid out and probed at 1 m intervals to establish thaw depth. In coarse-grained substrates, a single 10 m transect going through both polygon centres and trough was used and probed at 1 m intervals.

A local Digital Terrain Model (DTM) was built for each site using a backpack-mounted Kinematic Mobile LiDAR Scanner (KLS) developed by the Finnish Geospatial Institute (Kukko 2013). Each site was scanned by the GPS equipped KLS unit to collect extensive, high-resolution morphology data that has high vertical accuracy (within 2cm) and an absolute global position within 10 cm of the operator (Zanetti et al. 2018). The KLS instrument is outfitted with a Ring Laser Gyroscope to account for the movement of the operator (Kukko 2013) and scans up to 1 million points and 120 lines per second and as far as 150 m to the left and right of the instrument. This allows for rapid scanning of areas thousands of square metres of polygon terrain that results in dense point cloud data and DTMs of a higher resolution than previously found in the study area. The DTMs were used for detailed analysis of the geomorphology (e.g., shape, area) of the polygon networks around the Haughton impact structure.

A DJI Phantom 3 drone was used at each site to take a series of aerial images at a normal angle (90°) to the ground from an altitude of 30 m. Markers were used as ground control points to mark pre-recorded GPS points for georeferencing of the stitched mosaic in post-field image processing. The drone images are high resolution (12 megapixels) and allowed for video and images to be used for context and aerial imagery in the absence of a helicopter.

Point cloud and raster data were extracted from the KLS and imported into ESRI ArcMap software (ArcGIS 10.5.1). The "LAS to Raster" tool in ArcMap was used to convert the LiDAR data into high-resolution DTMs of each site. The resulting DTMs are fully georeferenced with a resolution of 2–5 cm/pixel, one of the highest resolutions produced of this field site. The DTMs were used as the basis of a morphology and morphometry analysis in ArcGIS software. ArcGIS was used as the primary lab tool for geomorphological mapping and analysis of each field site. Methods for the digitization of the polygons was adapted from Ulrich et al. (2011) where a similar technique was used to collect aspects of polygon morphology including polygon area, size, perimeter, and circularity. Each polygon network was manually digitized by tracing along the centrelines of clear contraction cracks and troughs. Polygons were represented where an area was fully enclosed by contraction cracks. Metrics were calculated in ArcGIS to characterize each site in detail and are summarized in Table 1.

Table 1: Description of polygon geomorphology metrics that were calculated for each polygon within the study areas. See Figure 2.5.

Metric	Description
Area (m^2)	The total area with a polygon
Perimeter (m)	The total length of all polygon sides
Length (m)	The longest diameter of a polygon
Width (m)	The shortest diameter of a polygon
Circularity	$4\pi A/P^2$ Where A is polygon area and P is polygon perimeter. 0 represents an elongated ellipse and 1 represents a circle
Aspect Ratio	W/L. Where W is width and L is length

An ArcMap tool developed by Brooker et al. (2018) was used to streamline this process and produce accurate metrics for each site. The polyline shapefile representing the polygon cracks and troughs was input into the tool. The tool produces a shapefile representing the enclosed polygons and their vertices (Fig. 2.5). The attribute table for the resulting shapefile contains the metrics for each polygon. Due to morphological differences between lcp and hcp, other features such as the high centres of the hcp and the raised rims of the lcp were mapped as needed. For example, the hcp at the Haughton Formation were traced along the centrelines of the troughs as well as the outer edges of the degraded high centres to accurately represent both main components of the morphology. The lcp at Lake Orbiter

were also traced along the centreline of the contraction crack troughs. Here, the depressed low centre was also mapped to show the polygon interior as well as the centreline of the raised shoulders around the interior to showcase the full morphology of the lcp. Lake Comet, having hcp without degraded centres, was mapped only along the centreline of troughs. Other periglacial features, including any smaller patterned ground, were also mapped. At each site, the intersections of contraction cracks, also called polygon junctions, were marked to show the vertices of the polygon networks clearly. The vertices were marked as being an intersection with three rays or four rays extending from them (Fig. 2.5).

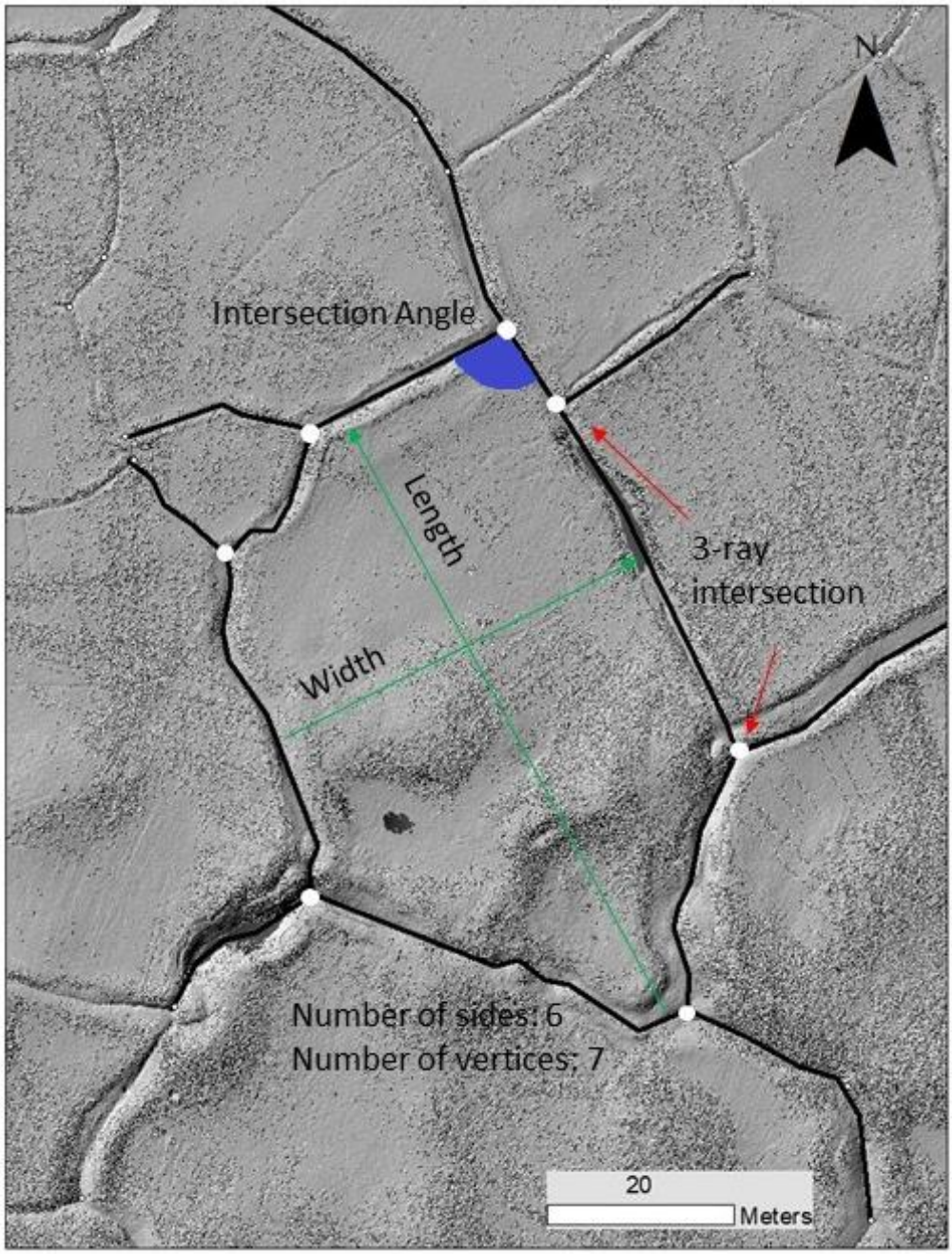

Figure 2.5: An example of the parameters extracted using the ArcMap polygon tool in a lcp at Lake Orbiter. The polygon centre is outlined by the traced trough lines. The polygon centre is the area contained within the trough lines and the length of the trough lines is the perimeter. The white dots represent the vertices where trough lines meet. The intersection type, polygon length and width, and trough intersection angles are noted in blue. Other parameters such as circularity are calculated using the values extracted by the ArcMap tool. Image modified after Ulrich et al. 2011 and Brooker at al. 2018

2.5 Results

The three study sites were characterized and mapped to distinguish their polygon networks resulting in a total of 223 polygons. An overview of the main characteristics of each site are summarized in Table 2. The polygon attributes analysed from the DTMs and mapping tools are presented in Table 3.

Table 2: An overview of the main physical characteristics of each polygon network.

Location	Haughton Formation	Lake Comet	Lake Orbiter
Average Elevation (meters above sea level)	140	195	180
Polygon Type	High Center	High Center	Low Center
Number of Polygons	138	25	60
Total Polygonized Area (m^2)	25969.7	51257.1	61663.9
Number of Trough Intersections	194	56	116
Average Trough Width (m)	3.8	5.9	2.3
Average Trough Depth (m)	0.53	0.71	0.33
3-ray intersections (%)	84.5	98.3	92.2
4-ray intersections (%)	15.5	1.7	7.8
Substrate	Unconsolidated, miocene aged plaeolacustrine sediments. Homogeneous, fine-grained, dolomite-rich sands and silts.	Blocky, coarse Allen Bay Formation dolomite frost shattered in situ with centimetre to decimetre sized clasts and finer throughout	Glaciofluvial sediments originating from Allen Bay dolomite. Gravel, sand and some fine grains throughout subsurface.

Table 3: Overview of statistics for attributes of each site from ArcMap polygon tool analysis. Metrics are described in Table 1. Standard deviation abbreviated to SD.

		Haughton Formation	Lake Comet	Lake Orbiter
Area (m^2)	Min	16.3	814.7	86.4
	Max	817.8	5460	6039
	Mean	188.2	2050.3	1233.3
	Median	170.6	1661	798.5
	SD	124.9	1080.6	1161.4
Perimeter (m)	Min	17.8	114.5	38.4
	Max	131.8	284.7	352.8
	Mean	53.2	176.8	132.5
	Median	54.2	168.1	117.4
	SD	17.8	43.9	60.9
Length (m)	Min	4.6	40.3	14.8
	Max	53.2	101	123.2
	Mean	19.8	63.7	47.7
	Median	20.3	60.2	42.1
	SD	6.8	16.3	21.3
Width (m)	Min	3.9	26.8	10
	Max	26.5	77.7	81.9
	Mean	12.6	43.3	32.8
	Median	12.8	39.3	28.4
	SD	4.6	12.3	15.3
Circularity	Min	0.54	0.63	0.57
	Max	0.89	0.89	0.86
	Mean	0.75	0.78	0.75
	Median	0.80	0.79	0.75
	SD	0.06	0.05	0.07
Aspect Ratio	Min	0.28	0.53	0.45
	Max	0.86	0.88	0.87
	Mean	0.64	0.68	0.69
	Median	0.60	0.67	0.69
	SD	0.10	0.08	0.01

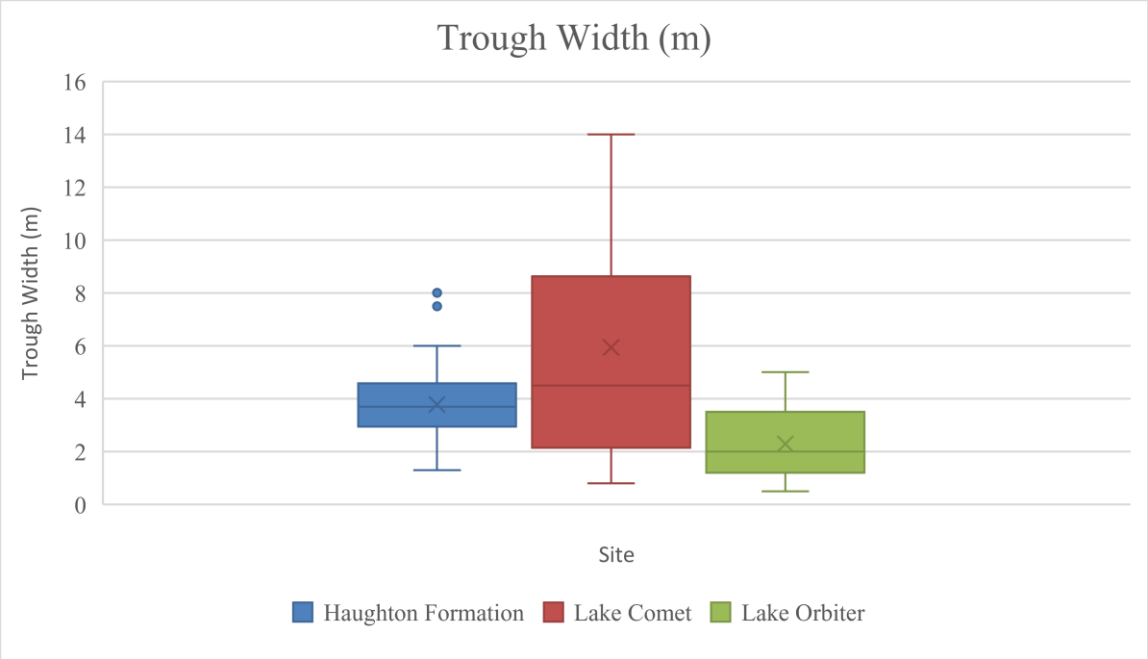

Figure 2.6: Box plot for trough widths from randomly selected samples at each study site. The bottom of the box represents the first quartile and the top of the box represents the third quartile, the "x" represents the mean, the transversal line within the box represents the median, the whiskers represent the maximum and minimum values, and the dots represent outliers.

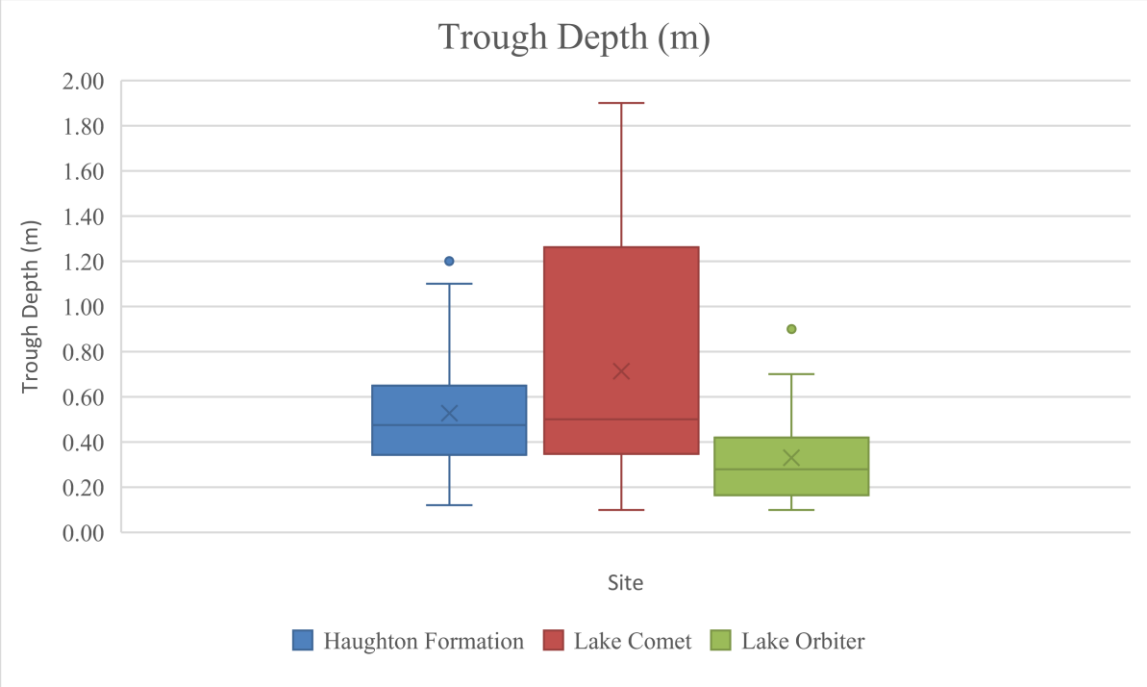

Figure 2.7: Box plot for trough depths from randomly selected samples at each study site. The top of the box represents the first quartile and the bottom of the box represents the third quartile, the "x" represents the mean, the transversal line within the box represents the median, the whiskers represent the maximum and minimum values, and the dots represent outliers.

2.5.1 The Haughton Formation

The flat areas of the Haughton Formation ubiquitously display high-centred ice wedge polygons that are well defined (Figs. 2.2c, d). The polygons are formed in an extended, flat area of unconsolidated, fine paleolacustrine sediments on a lower terrace of the Haughton Formation. The polygons in the Haughton Formation are an average of 19.8 m across (Table 2) and display a geometrically regular and mostly orthogonal pattern. The polygon rims are heavily degraded along the edges of the high centres that are bordered by troughs that are 3.8 m wide (SD = 1.5 m) and 0.53 m deep (SD = 0.26 m) on average (Figs. 2.6, 2.7) (Table 2). The polygon network mapped contains a total of 138 hcps covering an area

of 25,970 m^2 (Table 2). The polygon surface area ranges from 16.3 to 817.8 m^2 (Fig. 2.8) with an average polygon area of 188 m^2 (SD = 125 m^2) (Table 3).

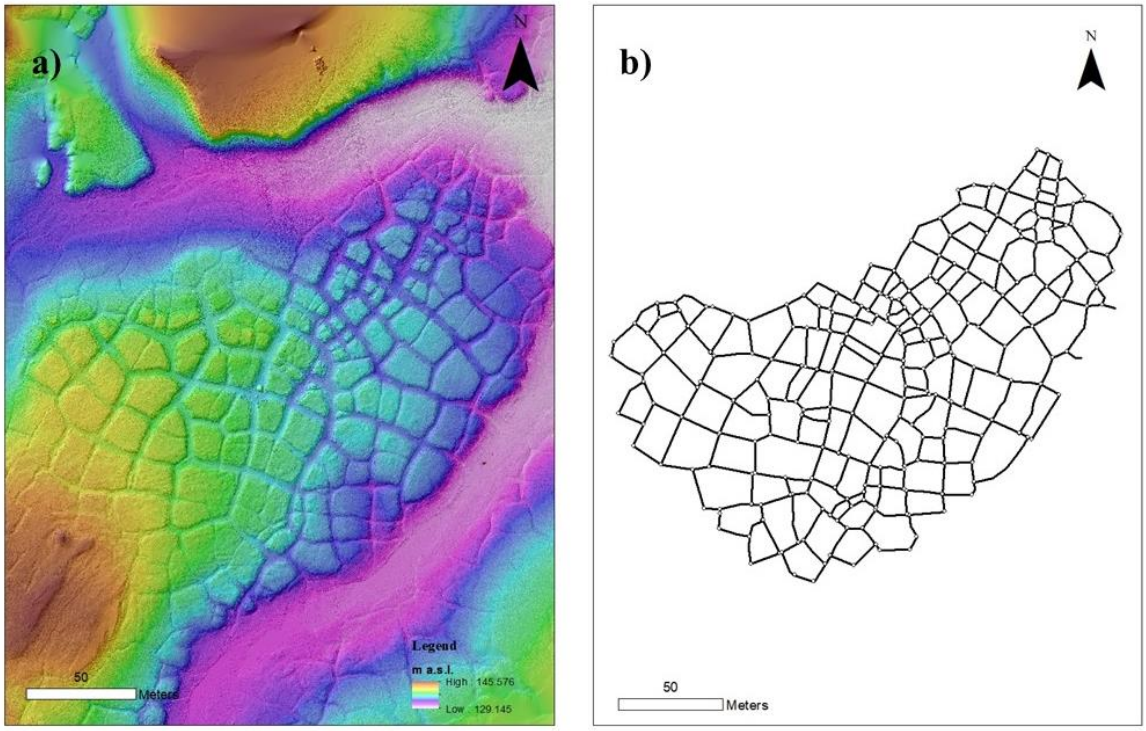

Figure 2.8: a) An elevation colourized shaded relief image based on a DTM derived from a KLS scan of the Haughton Formation polygon network and study site. b) A simplified representation of the Haughton Formation polygon trough lines and vertices displaying the polygon network and orthogonality.

The substrate of the Haughton Formation field site is primarily sand with other fines of a light to medium brown colour. At 40 cm depth in the centre of a hcp, a dark-brown organic-rich horizon was found that is seen clearly along the crumbling edges of the polygon centres (Fig. 2.9a). The soil pit was dug to 56 cm depth at which point ice-rich frozen ground was observed. Within the trench dug across the trough the subsurface displayed a fine brown sandy layer that is consistent all the way down to the frozen ground at 42 cm depth. A brown sandy layer is present above and below the organic-rich layer (Fig. 2.9b). The ground at the bottom of the trench was found to be ice-rich and although the boundaries of

the ice-wedge were not clearly observed, the subsurface at this depth was more ice than soil. In July 2017 the thaw depth was observed to be 56 cm in the polygon centre soil pit and 42 cm in the trough trench. An average of all thaw depth measurements from both the probed transects and soil pits was of 45.2 cm depth.

There is small (5–10 cm) sorted polygon patterned ground within the centres of the large hcp. The small sorted patterns were only observed in the hcp centres, not the troughs. The small patterned ground appears similar to mud cracks and displays minor sorting of small (~1cm) pebbles along the cracks of the small polygons (Fig. 2.9c).

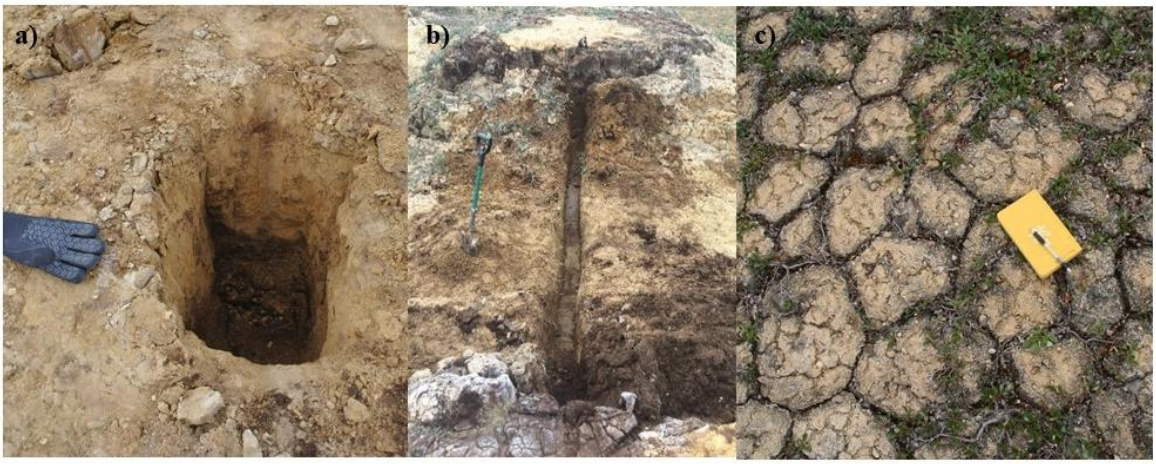

Figure 2.9: a) Soil pit dug in the centre of a hcp in the Haughton Formation. The first 40 m of the pit show fine brown sand–silt layer. Below that is the dark, porous, organic-rich layer continuing to the frozen ground at 56 cm. b) A 5.5 m trench dug from one hcp edge to another through a trough. The dark organic-rich layer is seen on the edge and another brown layer beneath it in the trough. Shovel for scale. c) Small patterned ground found within the centre of a hcp in the Haughton Formation. The patterns are similar to mud cracks and have minor sorting of pebbles in the cracks.

2.5.2 Lake Comet

Lake Comet displays large hcp polygons formed within frost shattered Allen Bay dolomite blocks and cobble to gravel-sized coarse sediments surrounding the lake. The hcps are well

defined on the flat top and gentle slopes of a hill that spans most of the south shore of the lake (Fig. 2.3). The polygons at Lake Comet are geometrically regular and display a mostly orthogonal pattern throughout the network. The orthogonal pattern is slightly offset and displays primarily 3-ray trough intersections, with almost no 4-ray (X shaped) intersections. The high centres of the polygons are raised and somewhat rounded with no raised rim. The hcps are bordered by degraded shoulders (Figs. 2.3a, b) and troughs 5.9 m wide (SD = 4.0 m) (Fig. 2.6) and 0.71 m deep (SD = 0.50 m) on average (Fig. 2.7) (Table 2). The troughs closest to the lake are much more heavily degraded and are as wide as 13 m and as deep as 1.5 m. In some cases, the deeper polygon junctions hosted pools of water. The hcps are 40–60 m across and range from 815 to 5,460 m^2 in area with an average size of 2,050 m^2 (SD = 1081 m^2) (Table 3). The polygon network map (Figs. 2.10a, b) contains 25 hcp covering an area of 51,257 m^2 (Table 2).

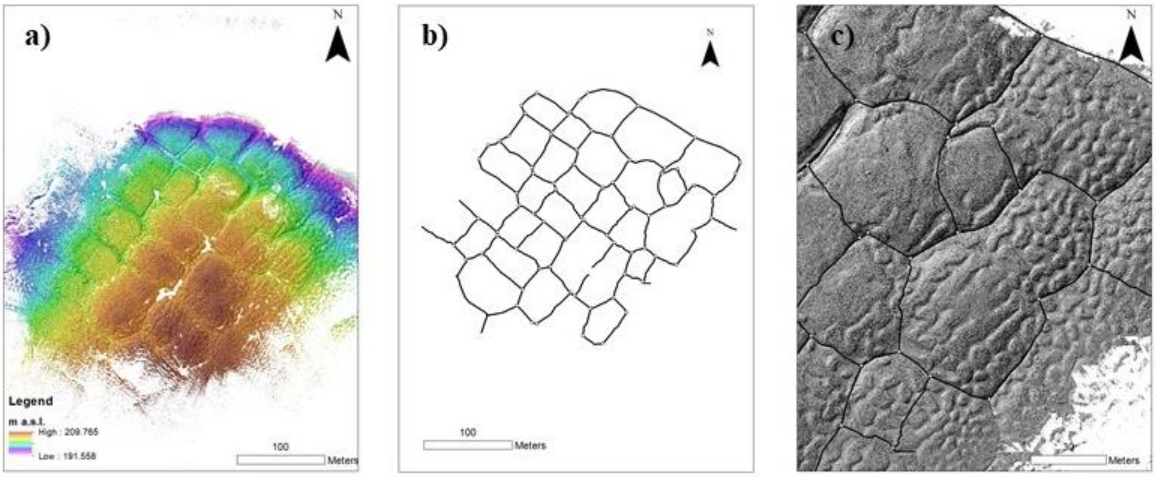

Figure 2.10: a) An elevation colourized shaded relief image based on a DTM derived from a KLS scan of the Lake Comet polygon network and study site. b) A simplified representation of Lake Comet polygon trough lines and vertices displaying the polygon network and orthogonality. c) Zoom image of the lobate patterned ground present on the gentle slopes of the Lake Comet polygon network.

The substrate at Lake Comet is coarse-grained at the surface but transitions to finer, sand-sized sediments 5–10 cm below the surface. The block field surface is heavily fractured

and rich in gravel-sized grains with the finer, sandy subsurface visible in some areas (Fig. 2.3a). Large, angular clasts continue to a depth of 5–10 cm after which the subsurface displays a finer-grained matrix with gravel throughout for ~15 cm. Below 40 cm the subsurface becomes gravelly with fine sediments and large cobbles throughout. The soil pit became too challenging to continue digging past 48 cm due to large clasts and frozen ground. Therefore, the thaw depth is estimated to be at minimum 40 cm on 27 July 2017.

Lobate, irregular patterned ground was observed within many polygon centres, localized mostly on the sloped surfaces on the southern side of the lake (Fig. 2.10c). The patterned ground lobes range in size and shape across the slope and do not display obvious sorting. The more circular forms are relatively uniform at ~5 m across and the elongated forms are 3–5 m across and upward of 15 m long. The patterns do not appear as frequently on the top of the hill and when present, are found only within the polygon troughs.

2.5.3 Lake Orbiter

Lake Orbiter displays flat to low-centred ice wedge polygons continuously throughout the large, relatively flat plain of gravel to cobble-sized clasts. The Lake Orbiter plain has two distinct sections, the southern section which contains subtle mounds and depressions and the northern section which is flatter (Fig. 2.4d). Some of the southern section terrain variations appear to be in relation to polygon centres (depressions) and rims (mounds). However, some large polygons have mounds within the centres as well. The polygons are mostly geometrically irregular in the southern section of the plain and are the largest in the site (50–80 m) (Fig. 2.11b). The majority of the large southern polygon junctions are non-orthogonal and have wider troughs (~2 m) (Figs. 2.11a, b). To the north of the plain, the polygons become flatter and smaller (15–30 m) with more narrow troughs (~1 m) (Fig. 2.11b). The polygons here also become more geometrically regular and display more orthogonal junctions (Figs. 2.11a, b). The polygons across the Lake Orbiter site are flat to low-centred with raised rims (10–20 cm) and have troughs that are narrower (2.30 m, SD= 1.1 m) (Fig. 2.6) and shallow (0.33 m, SD = 0.20 m) on average (Fig. 2.7) than the other sites. The low-centred morphology is the most exaggerated in the southern area of Lake

Orbiter where some of the polygon troughs become deeper and wider and the rims become larger (Fig. 2.11a). These lcp have large, rounded rims up to 80 cm high and troughs that are up to 6 m wide and ~50–70 cm deep, filled with water. In some large lcp both the centres and troughs contained shallow pools of water with dark cyanobacterial mats. Other troughs closer to the lake had water running through them towards the lake. The polygon network contains 60 polygons covering 61,664 m^2 (Table 2). The lcp range in size from 86 to 6039 m^2 with an average size of 1233 m^2 (SD = 1161.4 m) (Figs. 2.11a, b) (Table 3).

One soil pit was dug in the centre of a polygon and another in a wide trough (Figs. 2.12a, b). Both pits offered similar results although the pit in the trough contained a greater proportion of fine, sand-sized sediments. In the centre pit, the cobble and gravelly surface continued to 15–25 cm depth. Beyond 25–30 cm the substrate became a sandy-gravel matrix. In the trough pit the cobble and gravel went to 10 cm depth followed by a finer matrix still rich in gravel going from 10–30 cm depth. On 26 July 2017 the thaw depth is estimated to be 32–40 cm as both pits went to 32–40 cm depth where the gravel became too frozen to dig further.

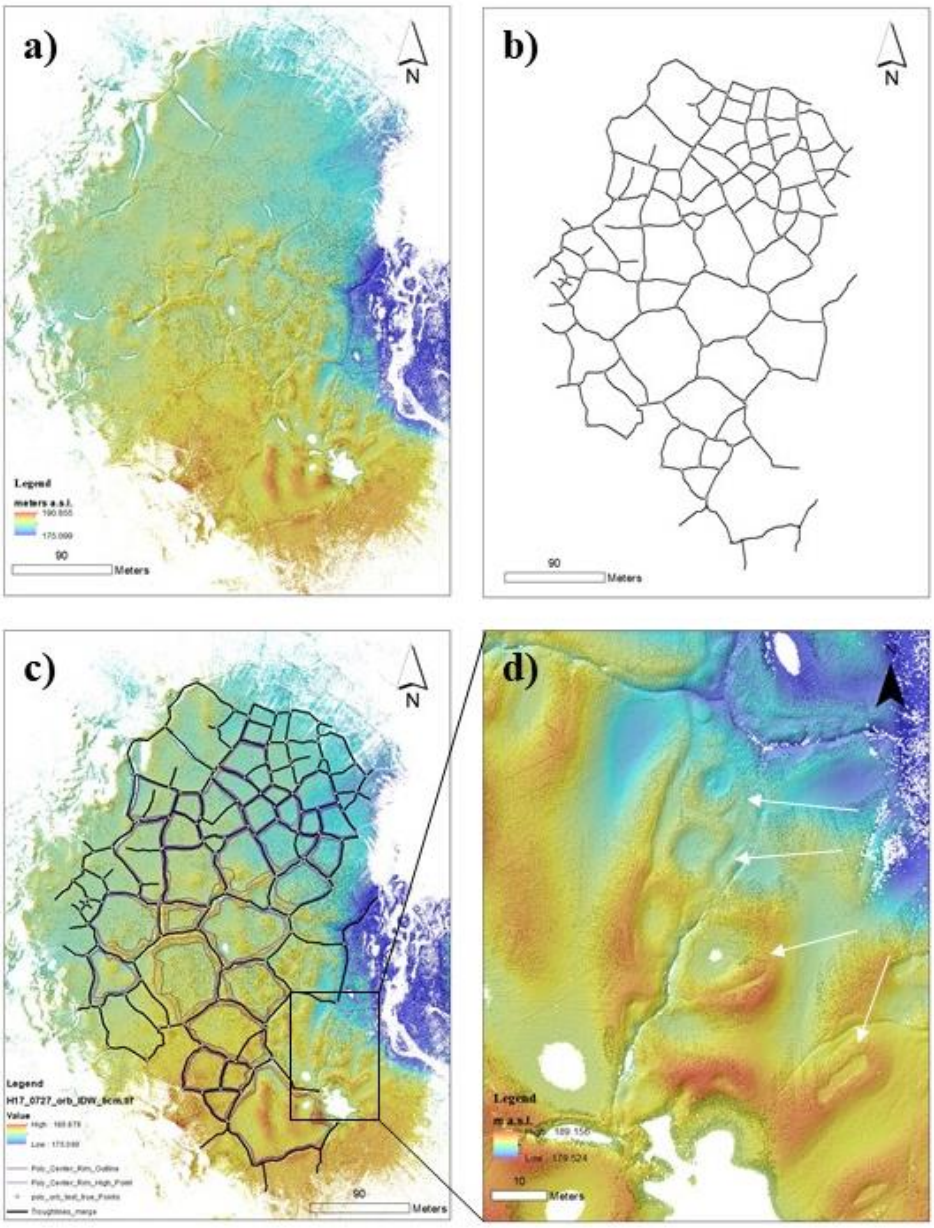

Figure 2.11: a) An elevation colourized shaded relief image based on a DTM derived from a KLS scan of the Lake Orbiter polygon network and study site. b) A simplified representation of Lake Orbiter polygon trough lines and vertices displaying the polygon network and orthogonality. c) The Lake Orbiter site mapped using ArcGIS. The base map made from the KLS is coloured to represent topography. The main trough lines, as well as the lcp shoulders and rims, are mapped as this is the only site that displays them. d) A zoomed image of the Lake Orbiter base map made from the KLS coloured to represent topography. The circular patterned ground, shown by the arrows, is clustered in this part of the site and mostly form close to cracks.

The Lake Orbiter polygons are the only lcp in the study area and have specific features that are not found in the other sites. The lcp display raised rims throughout much of the site; although they are the most well-formed in the southern area (Figs. 2.11a, c). The depressed centres and the centre line of the raised rims were mapped to show the distribution of raised rims throughout the site (Fig. 2.11c). There is inconsistency due to the non-uniform ground surface and many polygons in the north and the west area lack raised rims. The LiDAR scans reveal a change in topography that is not obvious in regular aerial or satellite imagery. The topography is slightly higher in the southern section which matches the change in the morphology (size, orthogonality, rim formation) of the polygons (Fig. 2.11c).

Figure 2.12 a) Soil pit dug in the centre of a lcp at Lake Orbiter. The ground displays a coarse surface that transitions to a finer sand and gravel mix. b) Soil pit dug in a wide trough of a lcp at Lake Orbiter. The coarse surface gives way to a sandy matrix at a shallower depth than in the polygon centre.

A cluster of circular patterned ground was observed along the shore of Lake Orbiter on the east side of the plain in the southern section (Fig. 2.11d). The patterns were not obvious in the field and were noticed to be circular patterned ground upon analysis of the LiDAR data. The patterns display a circular to ellipse morphology with raised rims and a depressed

centre, however, with no apparent sorting. The forms range significantly in size and occur both isolated (not touching another form) or in a line along a trough crack. The forms occurring in a line are consistently 5–6 m across while others that are more isolated are 10–23 m across.

2.6 Discussion

Our observations demonstrate that while the three study sites on Devon Island all display well-formed polygon networks, each site shows differing surface morphology. Each site displays unique combinations of polygon characteristics, such as large, non-orthogonal lcp at low lying Lake Orbiter and large, orthogonal hcp on a hill at Lake Comet. Differences were observed in sizes, orthogonality, and shape of the polygons (Figs. 2.8, 2.10 and 2.11 and Tables 2 and 3). We propose that the differences in morphology are driven mainly by substrate and stage of evolution, with factors such as vegetation cover, topography, and water availability, playing a more minor role(s). These factors are discussed in the following sections.

2.6.1 Relationship of Substrate and Polygon Evolution to Morphology

Previous work on periglacial morphology has shown a link between substrate characteristics and surface morphology (e.g., Drew and Tedrow 1962; Lachenbruch 1962; Washburn 1980; Romanovskji 1985). In coarse-grained substrates, a lower temperature is needed to cause cracking resulting in a trend toward hcp over lcp as ice-wedges degrade. With respect to grain size, homogeneous substrates are likely weaker than heterogeneous substrates causing cracks to occur more frequently and closer together. Over time, less cracking may occur in homogeneous substrates because the initial cracks reduce the amount of weakness in the frozen ground (Lachenbruch 1962; Romanovskij 1985). The Haughton Formation in the western side of the Haughton impact structure displays degraded high-centred polygons within a thick layer of lacustrine sediments (Fig. 2.2). The substrate is fine-grained and compositionally homogeneous (Fig. 2.9a) (Hickey et al. 1988)

with polygons that are small to medium-sized relative to the other sites, orthogonal and high-centred. Based on the level of degradation, the polygons are potentially in a later stage of development than the polygons observed at the other sites. The Lake Comet site has a coarse-grained surface with a likely compositionally homogeneous substrate of poorly sorted blocks to sand-sized sediments (Fig. 2.3a). The angular, blocky surface displays large, orthogonal hcp with deep troughs that vary in size, especially those that are adjacent to the lake (Figs. 2.3c, d), suggesting ice-wedge degradation that is affected by thermal erosion in places. The Lake Orbiter site is a coarse-grained surface with sub-rounded to sub-angular cobbles throughout (Fig. 2. 4a). The substrate is compositionally heterogeneous with sand-sized sediments strata in the subsurface (Fig. 2.12). This site displays a wide range of polygon sizes including some of the largest polygons of the three sites. Many of the largest polygons trend towards low-centredness. This suggests that these polygons are stable and at an earlier stage of development than the other two sites. The raised rims typical of lcp are the product of material being moved up from ice-wedge growth as well as moved from the centre toward the sides (Mackay 1980, 2000; French 2007) but some polygons with raised rims have large gaps in the rims (Fig. 2.11a). This may be due to ground disturbance, thermal irregularities or a lack of material.

The Haughton Formation has the highest number of, and the smallest sized, polygons of the three sites (Table 3), all formed in a fine, well-sorted homogeneous substrate. The site also displays less obvious secondary cracking (Fig. 2. 9a). These observations align with the work of Ulrich et al. (2011) who found the smallest polygons of the study in homogeneous silty deposits in the lower Adeventdalen in Svalbard, Norway. The observations are also supported by the relationship between homogeneous substrates and smaller distances between cracks due to higher ground ice content and thermal stress as well as substrates becoming less weak as primary cracks occur (e.g., Lachenbruch 1962, 1966). Coarse, heterogeneous material has lower thermal stress and is stronger causing contraction cracks to occur further apart as there are fewer points of weakness for cracks to propagate from (Lachenbruch 1962, 1966). Based on the work of Lachenbruch (1962, 1966), the large hcp are less likely to occur in the homogeneous material of the Lake Comet site; however, the poorly sorted substrate and large blocks at Lake Comet likely affect the stresses in the ground causing large hcp. The largest polygons of the study are found in

the southern section of Lake Orbiter; although the polygons do decrease in size going north (Figs. 2.11a, b). Previous work suggests that large polygons form in coarse-grained substrates (Lachenbruch 1962, 1966); however, since the polygons are smaller to the north, there may be a change in grain size or homogeneity in the Lake Orbiter substrate. The topography is slightly higher in the southern end which matches the change in the morphology of the polygons (Fig. 2.11a). This could potentially be the result of changes in sediment influx from the surrounding streams over time.

Hcps are observed as both the average smallest polygons observed (at the Haughton Formation) and the average largest (at Lake Comet) (Table 2). Lake Comet and Lake Orbiter are both course-grained substrates but display hcp and lcp respectively. Lake Orbiter and the Haughton Formation are both flat, low lying areas but display hcp and lcp respectively. Our findings show that not all of the study sites on Devon Island align well with previous work described above on homogeneity and topography as determining factors in polygon morphology, showing that other factors such as grain-size must be considered.

2.6.2 Orthogonality and Intersection Types

Contraction cracks occur along areas of weakness in newly frozen ground due to a complex yet mostly random distribution of stresses (Black 1952; Lachenbruch 1966;). The stresses and weaknesses in the ground will determine how and where cracks will intersect and thus, how orthogonal (90° intersections) a polygon network will be (Lachenbruch 1962, 1966;). Orthogonal networks likely form through the ongoing division of polygons while non-orthogonal networks form through continuous, random branching of cracks (Lachenbruch 1962; Plug and Werner 2001). It is thought that polygon networks mostly trend towards being orthogonal over time (Lachenbruch 1966; Plug and Werner 2001); although the reasons why networks may be non-orthogonal are not well constrained. That being said, previous work suggests that polygons found in homogeneous substrates typically display non-orthogonal patterns while polygons found in heterogeneous substrates often display

orthogonal patterns (Lachenbruch 1962, Christiansen 2005; French 2007). This is the opposite of what we have described.

The Haughton Formation polygons display an orthogonal pattern throughout the site (Fig. 2.8). The polygons are closest to an orthogonal pattern displaying mostly 90° angles as described in French (2007) as opposed to a random orthogonal pattern. As noted above, orthogonal patterns within homogeneous substrates is not typical. Throughout the Lake Comet site, the polygons also display an orthogonal pattern in poorly-sorted, coarse-grained homogeneous sediments (Figs. 2.10a, b), which is similar to the orthogonal pattern seen at the Haughton Formation in fine-grained, homogeneous sediment. Our observations of the Lake Comet are not in keeping with the accepted interpretation that non-orthogonal polygon networks occur in homogeneous substrates (Lachenbruch 1962, French 2007). However, the poorly sorted substrate and the presence of extended felsenmeer may influence the orthogonality. The presence of orthogonal polygons at the Haughton Formation is somewhat unexpected. Models by Plug and Werner (2001) suggest that homogeneous substrates are likely to display equiangular intersections, although it is unclear if this only applies to 120° angles or 90°, orthogonal angles can also occur in the model. If the Haughton Formation network substrate had the stresses needed to form through the ongoing division of polygons, then according to Plug and Werner (2001) an equiangular (90°), orthogonal system would be expected in the homogeneous substrate. The orthogonal polygons at Lake Comet appear to be somewhere between a random orthogonal and somewhat oriented orthogonal pattern (French 2007). A few of the contraction cracks have formed perpendicular to the lake northeast of the polygon network but do not continue far into the polygon network (Fig. 2.10b). The polygons at the Lake Orbiter site are mostly geometrically irregular in shape have both non-orthogonal and mostly orthogonal arrangement within the site within the heterogeneous substrate. The most non-orthogonal polygons are also the largest in the southern section and the most orthogonal are the smallest in the northern section (Figs. 2.11a, b). The size and the orthogonality follow the same distribution across the study site which suggests there may

be a grain size or homogeneity change across the site north to south.

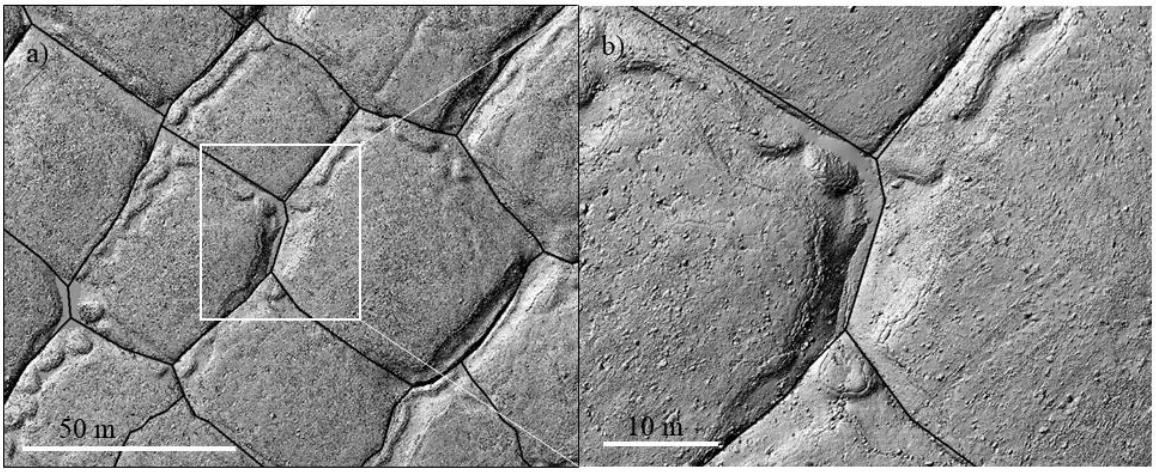

Figure 2.13: a) The Lake Comet site showing the mapped trough lines. b) A zoomed image of a) showing the three-ray intersections that frequently occur throughout the orthogonal Lake Comet polygon network.

It is generally accepted that a three-ray intersection often have mostly equal angles of 120° in between rays pointing to a non-orthogonal (hexagonal) network (Lachenbruch 1962; Plug and Werner 2001) and a four-ray intersection would have 90° between each ray suggesting an orthogonal network (Ulrich et al. 2011). Our observations show many 3-ray intersections in the three sites do not display equiangular 120° spacing and instead have a "T-shape" configuration with 180°, 90° and 90° spacing. At all three sites the dominant type of trough intersection was a three-ray intersection (Table 2); however; the Haughton Formation had the highest percentage of four-ray intersections at 15%. Both Lake Comet and Lake Orbiter have over 90% three-ray intersections of both types (Table 2). While Lake Comet is orthogonal, most intersections do not form a four-ray "X" intersection and instead are actually two, three-ray intersections forming very close together (Fig. 2.13). To the best of the author's knowledge, this intersection morphology has not been named or reported on specifically in the literature, however, it may be caused by the two three-ray contraction junctions initiating almost simultaneously instead of one occurring then the other, which would be more likely to manifest as a four-ray intersection (French 2007).

Lake Orbiter is mostly non-orthogonal (Figs 2.11a, b), and the high percentage of three-ray intersections suggest more random formation of the polygon network (Plug and Werner 2001), even in the section of Lake Orbiter that is more orthogonal.

The study sites, in general, do not align well with many of the expected relationships between polygon morphology and substrate. For example, previous work suggests that a non-orthogonal polygon pattern is expected to be found within a homogeneous substrate and an orthogonal polygon pattern is expected to be found in a heterogeneous substrate (Lachenbruch 1962; French 2007). Our sites do not align with such observations as the Haughton Formation and Lake Comet are orthogonal in well-sorted homogeneous and poorly-sorted homogeneous substrates respectively and Lake Orbiter has both orthogonal and non-orthogonal polygons in a heterogeneous substrate. This is not uncommon as work by Ulirch et al. (2011) found orthogonal polygon networks in homogenous substrates in Svalbard and work by Halitgin et al. (2012) found oriented orthogonal polygon network on a fine-grained floodplain deposit east of the Haughton impact structure. Findings by Dutilleul et al. (2009) through SPPA suggests that homogeneous substrates may have a more regular distribution of weaknesses as opposed to random distribution suggested by Lachenbruch (1962), resulting in more regular point patterns and ultimately, more orthogonal networks. Our results also support that the orthogonality of a polygon network is not tied only to substrate.

2.6.3 Polygon Troughs and Degradation

The large, wide troughs in the Haughton Formation polygon network suggest erosion and ice-wedge melt due to a significant period of inactivity. This is consistent with the more heavily degraded polygons at the Haughton Formation with the deepest troughs being observed on one of the lower-most terraces of the area. A higher terrace displayed hcp of similar size and orthogonality but with more shallow troughs and less degraded edges. The excess degradation may be a result of the thermal erosion of the fine-grained substrate and the relatively high amount of water that pools and flows through the low-lying terrace (Jorgenson et al. 2006). The increased depth of the troughs suggests higher temperatures

in the ice wedges and the substrate directly surrounding them, possibly due to increased snow accumulation and insulation of the active layer (Abolt et al. 2018). The Lake Comet site displays mostly uniform trough depths throughout; however, the deepest, widest troughs are seen on the steepest slopes nearest to the lake. The increased drainage of water downslope toward the lake and subsequent thermal erosion may cause ice-wedges to degrade faster, thus deepening and widening the troughs more (e.g., Jorgenson et al. 2006, Fortier et al. 2007). The large troughs on the slope were found to border the smaller polygons at the site while the largest polygons were found to occur on the flatter hilltop where they had more shallow and narrow troughs. There is a relationship between trough width and slope here where we see that wider troughs occur on more pronounced slopes where more drainage and degradation are occurring. The lcps throughout Lake Orbiter have troughs that are mostly narrow and shallow compared to the other sites; however, there are troughs throughout the site that are much deeper and wider than the rest, much like Lake Comet. Such troughs contain deep pools of water or have water draining through them toward the lake. The troughs that contain water may contain ice-wedges that are no longer growing or stable and are beginning to degrade. There are significant inconsistencies in trough morphology within each of the study sites. Since all three sites experience similar climatic conditions, trough size and degradation are likely influenced the most significantly by site-specific topography, hydrology and slope, although the influence of substrate is not well constrained.

2.6.4 Polygon Shape Distribution

The shapes of the polygons are somewhat inconsistent throughout the study sites. The measured circularity is between 0.53 and 0.89 with the Haughton Formation having the minimum and maximum across the sites (Table 2). We suggest that the wide range in circularity may be influenced by the high degree of degradation (see above) occurring at the site. Lake Comet has the highest average circularity, likely due to the 3-ray nature of the majority of trough intersections. Our results show Lake Orbiter has a slightly lower value and, thus, the polygons trend toward more elongated. The lower value may be attributed to the general irregularity of the site as many large, irregular polygons are non-

orthogonal. However, overall the polygons across all sites trend towards being more equally sided than elongated as the minimum calculated circularity is 0.52 (0 = elongated and 1=circular). The aspect ratios are similar in all sites trending toward more square suggesting the polygons fall within the mid-range and are overall not elongated, not perfectly square and not circular. For the Haughton Formation and Lake Comet sites, these results are likely due to their overall orthogonal nature. At Lake Orbiter many of the polygons may be irregular and non-orthogonal, however they are not elongated, resulting in a trend toward square. The Haughton Formation holds the minimum value for aspect ratio while Lake Comet holds that maximum. While circularity and aspect ratio are useful in gaining insight into each site as a whole, the general shape of polygons does not appear to be closely linked to substrate as we observe a similar average value across the three sites.

2.6.5 Patterned Ground within Polygons

The patterned ground at the Haughton Formation are small, similar to mud cracks and have minor sorting of pebbles into boundaries of the small sorted polygons (Fig. 2.9c). The small patterns only occur on the raised polygon centres where the ground is the driest and small, frequent cracking can occur. These small patterns were only observed at the Haughton Formation and not at the other sites. The patterned ground at Lake Comet (Fig. 2.10c) and Lake Orbiter (Fig. 2.11d) are of a similar lobate to circular form. Are the patterns at both sites formed from similar processes but are at different stages of development? The Lake Comet patterns may be more evolved than the ones at Lake Orbiter since the polygons at Lake Comet are at a later stage of development than the polygons at Lake Orbiter. The patterns at Lake Orbiter have a more distinct circular form and depressed centres though they are not sorted circles (Washburn 1980). The depressed centres could be the result of ice lenses melting or be similar to a collapsed or failed pingo (Mackay 1987). However, the clustering of the forms at Lake Orbiter and the apparent orientation along cracks (Fig. 2.11d) suggest that the patterns might be more related to thermal variation moving sediments from the inner circle outwards in the same way lcp rims are formed (Mackay 2000; French 2007). The factors influencing the formations of non-sorted, non-thermal contraction patterned ground is not well constrained. The differences in the inter-polygon

pattern ground at Lake Comet and Lake Orbiter further support that the sites have significant differences in factors influencing polygon morphology and may have implications surrounding the role of substrate in periglacial processes.

The apparent differences in each site indicate factors are influencing the morphology changes. The differences in the sites are mainly geology and substrate as well as topography. Yet we do not see the same patterns across sites that have similarities in geology or topography (e.g., the Haughton Formation and Lake Orbiter are low laying and have hcp and lcp respectively). Previous modelling work by Plug and Werner (2002) suggest that average climatic conditions may not be a major factor in polygon morphology as much as initial or extreme conditions, which aligns well with what we see in our observations on Devon Island where our sites experience similar long-term climatic conditions.

2.7 References

Abolt, C.J., Young, M.H., Atchley, A.L., and Harp, D.R. 2018. Microtopographic control on the ground thermal regime in ice wedge polygons. The Cryosphere, **12**: 1957–1968.

Abolt, C.J., Young, M.H., and Caldwell, T.G. 2017. Numerical modelling of ice-wedge polygon geomorphic transition. Permafrost and Periglacial Processes, **28**: 347–355.

Bernard-Grand'Maison, C., and Pollard, W.H. 2018. An estimate of ice wedge volume for a High Arctic polar desert environment, Fosheim Peninsula, Ellesmere Island. The Cryosphere Dscussions. https://doi.org/10.5194/tc-2018-29, in review, 2018.

Black, R.F. 1952. Polygon patterns and ground conditions from aerial photographs. No. 1; Photogrammetric Engineering & Remote Sensing; **18**: pp. 123–134

Black, R.F., 1976. Periglacial features indicative of permafrost: ice and soil wedges. Quaternary Research. **6**, 3–26.

Brooker, L.M., Balme, M.R., Conway, S.J., Hagermann, A., Barrett, A.M., Collins, G.S., and Soare, R.J. 2018. Clastic polygonal networks around Lyot crater, Mars: Possible formation mechanisms from morphometric analysis. Icarus, **302**: 386–406.

Christiansen, H.H. 2005. Thermal regime of ice-wedge cracking in Adventdalen, Svalbard. Permafrost and Periglacial Processes, **16**: 87–98.

Costard, F., Forget, F., Madeleine, J.B., Soare, R.J., and Kargel, J. 2008. The origin and formation of scalloped terrain in Utopia Planitia: Insight from a general circulation model. Lunar and Planetary Science Conference, **39th**: 1274 pdf. Available from http://www.lpi.usra.edu/meetings/lpsc2008/pdf/1274.pdf. [accessed 3 May 2018].

de Smet, W.H., Beyens, L. 1995. Rotifersfrom the Canadian High Arctic (Devon Island, Northwest Territories). Hydrobiologia 313/314: 29–34.Dobiński, W. 2011. Permafrost. Earth-Science Reviews, **108**: 158–169.

Drew, J.V., and Tedrow, J.C.F. 1962. Arctic Soil Classification and Patterned Ground. Arctic, **15**. doi:10.14430/arctic3563.

Dutilleul, P., Haltigin, T.W., and Pollard, W.H. 2009. Analysis of polygonal terrain landforms on Earth and Mars through spatial point patterns. Environmetrics, **20**: 206–220.

Dyke, A.S. 1998. Holocene delevelling of Devon Island, Arctic Canada: implications for ice sheet geometry and crustal response. Canadian Journal of Earth Sciences, **35**: 885–904.

Dyke, A.S. 1999. Last Glacial Maximum and deglaciation of Devon Island, Arctic Canada: Support for an Innuitian ice sheet. Quaternary Science Reviews, **18**: 393–420.

Environment Canada. Canadian climate normals, 1961–1990. Resolute. 2018. http://climat.meteo.gc.ca/climate_normals/.

Fortier, D., and Allard, M. 2004. Late Holocene syngenetic ice-wedge polygons development, Bylot Island, Canadian Arctic Archipelago. Canadian Journal of Earth Sciences, **41**: 997–1012.

Fortier, D., and Allard, M. 2005. Frost-cracking conditions, Bylot Island, eastern Canadian Arctic archipelago. Permafrost and Periglacial Processes, **16**: 145–161.

Fortier, D., Allard, M., and Shur, Y.L. 2007. Observation of rapid drainage system development by thermal erosion of ice wedges on Bylot Island, Canadian Arctic Archipelago. Permafrost and Periglacial Processes, **18**: 229–243.

French, H.M. 2007. The Periglacial Environment. 3rd ed. John Wiley, Chichester, UK

Friedman, J.D., Johansson, C.E., Oskarsson, N., Svensson, H., Thorarinsson, S., and

Williams, R.S. 1971. Observations on Icelandic polygon surfaces and palsa areas. Photo Interpretation and Field Studies. Geografiska Annaler. Series A, Physical Geography, **53**: 115–145.

Godin, E., Osinski, G. R., Harrison, T. Zanetti, M. 2018. Geomorphology of gullies at Thomas Lee Inlet, Devon Island, Canadian High Arctic. Permafrost and Periglacial Processes. (accepted)

Haltigin, T.W., Pollard, W.H., and Dutilleul, P. 2010. Comparison of ground- and aerial-based approaches for quantifying polygonal terrain network geometry on Earth and Mars via spatial point pattern analysis. Planetary and Space Science, **58**: 1636–1649.

Haltigin, T.W., Pollard, W.H., Dutilleul, P., and Osinski, G.R. 2012. Geometric evolution of polygonal terrain networks in the Canadian High Arctic: evidence of increasing regularity over time. Permafrost and Periglacial Processes, **23**: 178–186.

Haltigin, T.W., Pollard, W.H., Dutilleul, P., Osinski, G.R., and Koponen, L. 2014. Co-evolution of polygonal and scalloped terrains, southwestern Utopia Planitia, Mars. Earth and Planetary Science Letters, **387**: 44–54.

Hauber, E., Reiss, D., Ulrich, M., Preusker, F., Trauthan, F., Zanetti, M., Hiesinger, H., Jaumann, R., Johansson, L., Johnsson, A., Van Gasselt, S., and Olvmo, M. 2011. Landscape evolution in Martian mid-latitude regions: insights from analogous periglacial landforms in Svalbard. Geological Society, London, Special Publications, **356**: 111 LP-131.

Hickey, L.J., Johnson, K.R., and Dawson, M.R. 1988. The stratigraphy, sedimentology, and fossils of the Haughton formation: A Post-Impact Crater-Fill. Meteoritics, **23**: 221–231.

Jorgenson, M.T., and Osterkamp, T.E. 2005. Response of boreal ecosystems to varying modes of permafrost degradation 1. Canadian Journal for Res., **35**: 2100–2111.

Jorgenson, M.T., Shur, Y.L., and Pullman, E.R. 2006. Abrupt increase in permafrost degradation in Arctic Alaska. Geophysical Research Letters, **33**: 2–5.

Kukko, A. 2013. Mobile Laser Scanning – system development, performance and applications. Ph.D Thesis. Department of Real Estate, Planning and Geoinformatics, Aalto University, Helsinki, Finland. 247p.

Lachenbruch, A.H. 1962. Mechanics of thermal contraction cracks and ice-wedge

polygons in permafrost. Geological Society of America Special Papers, **70**.

Lachenbruch, A. H. 1966. Contraction theory of ice-wedge polygons: a qualitative discussion. In Proceedings of First International Conference on Permafrost, 11–15 November 1963, Purdue University, Lafayette, IN. Washington, DC, National Academy of Sciences, National Research Council, 63–71. (NRC Publication 1287.)

Lee, P., and Osinski, G.R. 2005. The Haughton-Mars Project: Overview of science investigations at the Haughton impact structure and surrounding terrains, and relevance to planetary studies. Meteoritics and Planetary Science, **40**: 1777–1787.

Lefort, A., Russell, P.S., Thomas, N., McEwen, A.S., Dundas, C.M., and Kirk Physikalisches, R.L. 2009. Observations of periglacial landforms in utopia planitia with the high resolution imaging science experiment (HiRISE). Journal of Geophysical Research E: Planets, **114**: 1–18.

Levy, J.S., Head, J.W., and Marchant, D.R. 2009a. Thermal contraction crack polygons on Mars: Classification, distribution, and climate implications from HiRISE observations. Journal of Geophysical Research E: Planets, **114**: 1–19.

Levy, J.S., Head, J.W., Marchant, D.R., Dickson, J.L., and Morgan, G.A. 2009b. Geologically recent gully-polygon relationships on Mars: Insights from the Antarctic Dry Valleys on the roles of permafrost, microclimates, and water sources for surface flow. Icarus, **201**: 113–126.

Mackay, J.R. 1972. The World of Underground Ice. Arctic, **62**: 1–22.

Mackay, J.R. 1980. Deformation of ice-wedge polygons, Garry Island, Northwest Territories. *In* Geological Survey of Canada Paper. 80–1A. 287–291

Mackay, J.R. 1987. Some mechanical aspects of pingo growth and failure, western Arctic coast, Canada. Canadian Journal of Earth Sciences, **24**: 1108–1119.

Mackay, J.R. 1990. Some observations on the growth and deformation of epigenetic, syngenetic and anti-syngenetic ice wedges. Permafrost and Periglacial Processes, **1**: 15–29.

Mackay, J.R. 1993. Air temperature, snow cover, creep of frozen ground, and the time of ice-wedge cracking , western Arctic coast. Canadian Journal of Earth Sciences, **30**: 1720–1729.

Mackay, J.R. 1999. Periglacial features developed on the exposed lake bottoms of seven

lakes that drained rapidly after 1950, Tuktoyaktuk Peninsula area, western Arctic coast, Canada. Permafrost and Periglacial Processes, **10**: 39–63.

Mackay, J.R. 2000. Thermally induced movements in ice-wedge polygons, western arctic coast: a long-term study. Géographie physique et Quaternaire, **54**: 41–68

Mackay, J.R., and Burn, C.R. 2002. The first 20 years (1978-1979 to 1998-1999) of ice-wedge growth at the Illisarvik experimental drained lake site, western Arctic coast, Canada. Canadian Journal of Earth Sciences, **39**: 95–111.

Mangold, N. 2005. High latitude patterned grounds on Mars: Classification, distribution and climatic control. Icarus, **174**: 336–359.

Mangold, N., Maurice, S., Feldman, W.C., Costard, F., and Forget, F. 2004. Spatial relationships between patterned ground and ground ice detected by the Neutron Spectrometer on Mars. Journal of Geophysical Research E: Planets, **109**: 1–6.

Marchant, D.R., Lewis, A.R., Phillips, W.M., Moore, E.J., Souchez, R.A., Denton, G.H., Sugden, D.E., Potter N., J., and Landis, G.P. 2002. Formation of patterned ground and sublimation till over Miocene glacier ice in Beacon Valley, southern Victoria Land, Antarctica. GSA Bulletin, **114**: 718–730.

Mellon, M.T. 1997. Small-scale polygonal features on Mars: Seasonal thermal contraction cracks in permafrost. Journal of Geophysical Research: Planets, **102**: 25617–25628.

Mellon, M.T., McKay, C.P., and Heldmann, J.L. 2014. Polygonal ground in the McMurdo Dry Valleys of Antarctica and its relationship to ice-table depth and the recent Antarctic climate history. Antarctic Science, **26**: 413–426.

Morse, P.D., and Burn, C.R. 2013. Field observations of syngenetic ice wedge polygons, outer Mackenzie Delta, western Arctic coast, Canada. Journal of Geophysical Research: Earth Surface, **118**: 1320–1332.

Osinski, G.R., Lee, P., Spray, J.G., Parnell, J., Lim, D., Bunch, T.E., Cockell, C.S., and Glass, B. 2005a. Geological overview and cratering model for the Haughton impact structure, Devon Island, Canadian High Arctic. Meteoritics and Planetary Science, **40**: 1759–1776.

Osinski, G.R., Spray, J.G., and Lee, P. 2005b. Impactites of the Haughton impact structure, Devon Island, Canadian High Arctic. Meteoritics and Planetary Science, **40**: 1789–1812.

Osinski, G.R., and Lee, P. 2005. Intra-crater sedimentary deposits at the Haughton impact structure, Devon Island, Canadian High Arctic. Meteoritics & Planetary Science, **40**: 1887–1899.

Osinski, G.R., Lee, P., Spray, J.G., Parnell, J., Lim, D., Bunch, T.E., Cockell, C.S., and Glass, B. 2005a. Geological overview and cratering model for the Haughton impact structure, Devon Island, Canadian High Arctic. Meteoritics and Planetary Science, **40**: 1759–1776.

Osinski, G.R., Spray, J.G., and Lee, P. 2005b. Impactites of the Haughton impact structure, Devon Island, Canadian High Arctic. Meteoritics and Planetary Science, **40**: 1789–1812.

Parnell, J., Bowden, S.A., Osinski, G.R., Lee, P., Green, P., Taylor, C., and Baron, M. 2007. Organic geochemistry of impactites from the Haughton impact structure, Devon Island, Nunavut, Canada. Geochimica et Cosmochimica Acta, **71**: 1800–1819.

Plug, L.J., and Werner, B.T. 2001. Fracture networks in frozen ground. Journal of Geophysical Research, **106**: 8599–8613.

Plug, L.J., and Werner, B.T. 2002. Nonlinear dynamics of ice-wedge networks and resulting sensitivity to severe cooling events. Nature, **417**: 929–933.

Romanovskji, N.N., 1985. Distribution of recently active ice and soil wedges in the USSR. In: Church, M., Slaymaker, O. (Eds.), Field and Theory; Lectures in Geocryology. University of British Columbia Press, Vancouver, pp. 154–165

Seibert, N.M., and Kargel, J.S. 2001. Small scale martain polygonal terrain: Implications for liquid surface water. Geophysical Research letters, **28**: 899–902.

Séjourné, A., Costard, F., Gargani, J., Soare, R.J., and Marmo, C. 2010. Polygon junction pits as evidence of a particularly ice-rich area in Utopia Planitia, Mars. Lunar and Planetary Science Conference, **41**: 2113.

Singleton, A.C., Osinski, G.R., Samson, C., Williamson, M.C., and Holladay, S. 2010. Electromagnetic characterization of polar ice-wedge polygons: Implications for periglacial studies on Mars and Earth. Planetary and Space Science, **58**: 472–481. Elsevier.

Soare, R.J., and Osinski, G.R. 2009. Stratigraphical evidence of late Amazonian periglaciation and glaciation in the Astapus Colles region of Mars. Icarus, **202**: 17–

21.

Thorsteinsson, R., and Mayr, U. 1987. The sedimentary rocks of Devon Island, Canadian Arctic Archipelago. Geological Survey of Canada Memoir, **411**: 1–182.

Ulrich, M., Hauber, E., Herzschuh, U., Härtel, S., and Schirrmeister, L. 2011. Polygon pattern geomorphometry on Svalbard (Norway) and western Utopia Planitia (Mars) using high-resolution stereo remote-sensing data. Geomorphology, **134**: 197–216. Elsevier B.V.

Washburn, A.L. 1980. Geocryology. A survey of periglacial processes and environments. The Blackburn Press, New Jersey.

Young, K.E., Van Soest, M.C., Hodges, K. V., Watson, E.B., Adams, B.A., and Lee, P. 2013. Impact thermochronology and the age of Haughton impact structure, Canada. Geophysical Research Letters, **40**: 3836–3840.

Zanetti, M., Neish, C.D., Kukko, A., Choe, B.H., Osinski, G.R., Tolometti, G., Fan, K., Maj, R., Heldmann, J. 2018. Surface roughness and radar scattering properties of volcanic terrain: geologic application of kinematic mobile LiDAR scanning. In Prodeedings from the 49th Lunar and Planetary Science Conference, The Woodlands, TX. (Abstract #2083).

Chapter 3

3 Conclusions and Future Work

The purpose of this work was to determine the factors that contribute to polygon morphology in different sites within the polar desert environment of Devon Island, where climatic conditions are currently relatively constant. Polygon morphology has implications for paleoenvironmental conditions, ground ice content and water availability for Earth and Mars. Few have examined the mechanisms behind differences in polygon morphology in High Arctic environments, (e.g., Ulrich et al. 2011), and causes for variations in morphology are not well constrained. Therefore, detailed work is needed to explore the factors that influence significant morphological differences in polygonal terrain. With high-resolution datasets (2–5 cm/pixel) of three polygonal terrain sites using KLS data (Chapter 2) in combination with fieldwork, each site was characterized in detail to determine the significant differences -between the sites that may influence the polygon morphology (Chapter 2).

3.1 Major Findings and Future Work

Findings from this work demonstrate the heterogeneity of polygon morphology and calls into question some previously assumed predictors, such as grain size and homogeneity. The study sites on Devon Island do not consistently conform to broad statements regarding how polygon morphology is reflected in specific substrates from previous works (e.g., Lachenbruch 1962, 1966; Romanovskij 1985; French 2007). There is considerable intra- and inter-site variability in morphology that does not correlate to a specific factor such as homogeneity, grain size or topography. High-centre, mostly orthogonal polygons were observed in both fine-grained, well sorted homogeneous substrate at the Haughton Formation and in coarse-grained, poorly sorted heterogenous substrate at Lake Comet. At Lake Orbiter, a network of both orthogonal and non-orthogonal polygons was observed as well as significant variation in low-centredness. The hcp at the Haughton Formation and the lcp at Lake Orbiter occur in low-lying areas while the hcp at Lake Comet occur on a local topographic high. Site-specific observations question the validity of assuming a global parameter to estimate polygon morphology. Our findings are supported by previous

work in High Arctic environments that found similar inconsistencies (e.g., Dutilleul et al. 2009; Ulrich et al. 2011; Haltigin et al. 2012). The inconsistencies in the relationship between polygon morphology and substrate are unexpected and may be explained by further work on substrate properties and on topography with the KLS.

High-resolution datasets created from the KLS have provided a higher level of detail in mapping and analysis of polygon networks than previously possible in the study region. The 2–5 cm/pixel resolution DTMs produced allowed for metrics such as trough depth and polygon size to be measured with a high degree of accuracy. The maps also allowed for minute features such as patterned ground and relatively recent contraction cracks not apparent in the field, to be identified. Smaller, inter-polygon patterned ground observed at the Lake Comet (Fig. 3.1a) and Lake Orbiter (Fig. 3.1b) study sites were found using the high-resolution dataset available from the LiDAR scans. In coarser scale imagery, these patterns were not well observed due to smoothing of the landscape which may have implications in the future when examining changes to polygonal terrain and other patterned ground over time. The distribution of the patterned ground at both sites is inconsistent and the mechanisms for formation were not constrained in this study. Further work on small, inter-polygon patterned ground such as the patterns observed on Devon Island is suggested to determine the importance of these patterns and what they may tell us about the periglacial processes occurring.

Our research has shown that the periglacial environment in and around the Haughton impact structure is dynamic and complex. We have focused on characterizing each of the study sites, reporting the details of their periglacial features and any inconsistencies with previous work. Each of the study sites has the potential for further meaningful study, as well as other sites around the Haughton impact structure and within polar desert environments. Due to the site-specific nature of polygon patterns in this region, we suggest exploring how combining measurements such as temperature variations, hydrology, topography and grain size distributions to gain a greater understanding of the geomorphology evolution. Such measurements would provide a more detailed profile for each site and may contribute additional information as to which factors have the most substantial influence on changes in morphology.

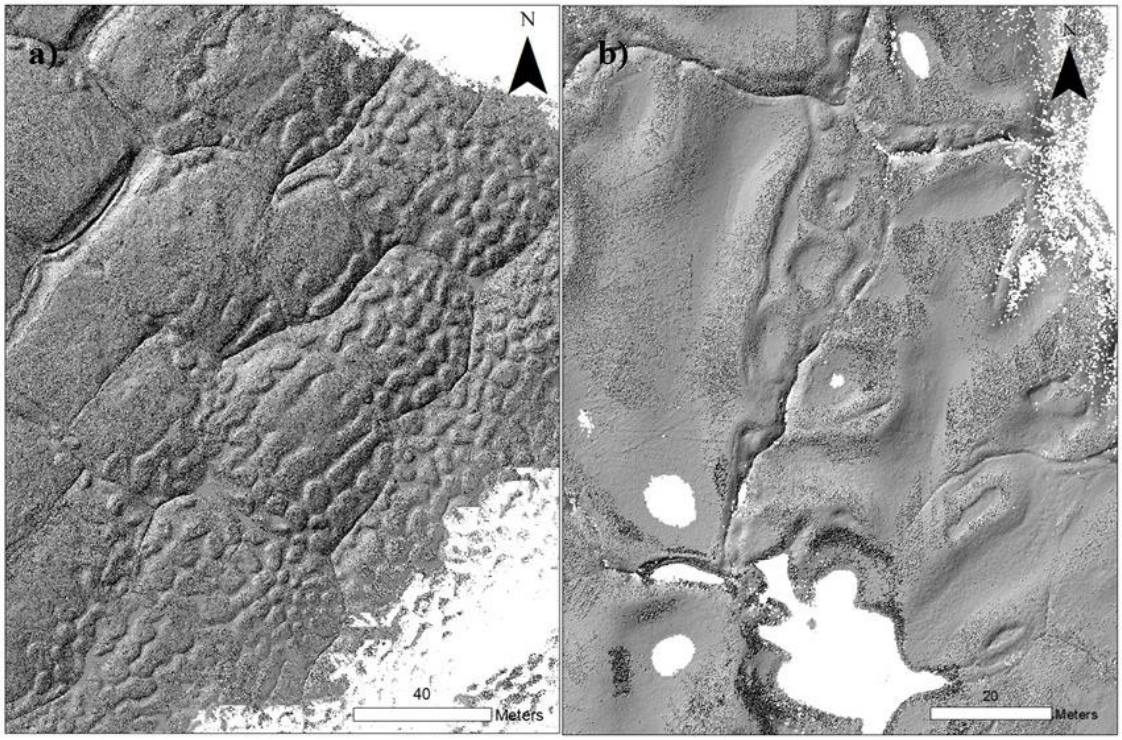

Figure 3.1: a) KLS data showing the lobate inter-polygon pattern ground at the Lake Comet site. b) KLS data showing the circular patterned ground at the Lake Orbiter site.

This study had three study sites with different topographic features, and we suggest the use of more study sites that display similar characteristics to parse out the differences between topographic and substrate controls. In addition, the extremely high-quality data derived from the KLS system may have uses beyond those reported in this work and should be used on more sites to learn more about the geomorphology of the sites as well as the capabilities of the KLS system. Larger scale processes, such as slope, coupled with micro-topographic features, such as trough depth, could provide insight into the role of different scale influences.

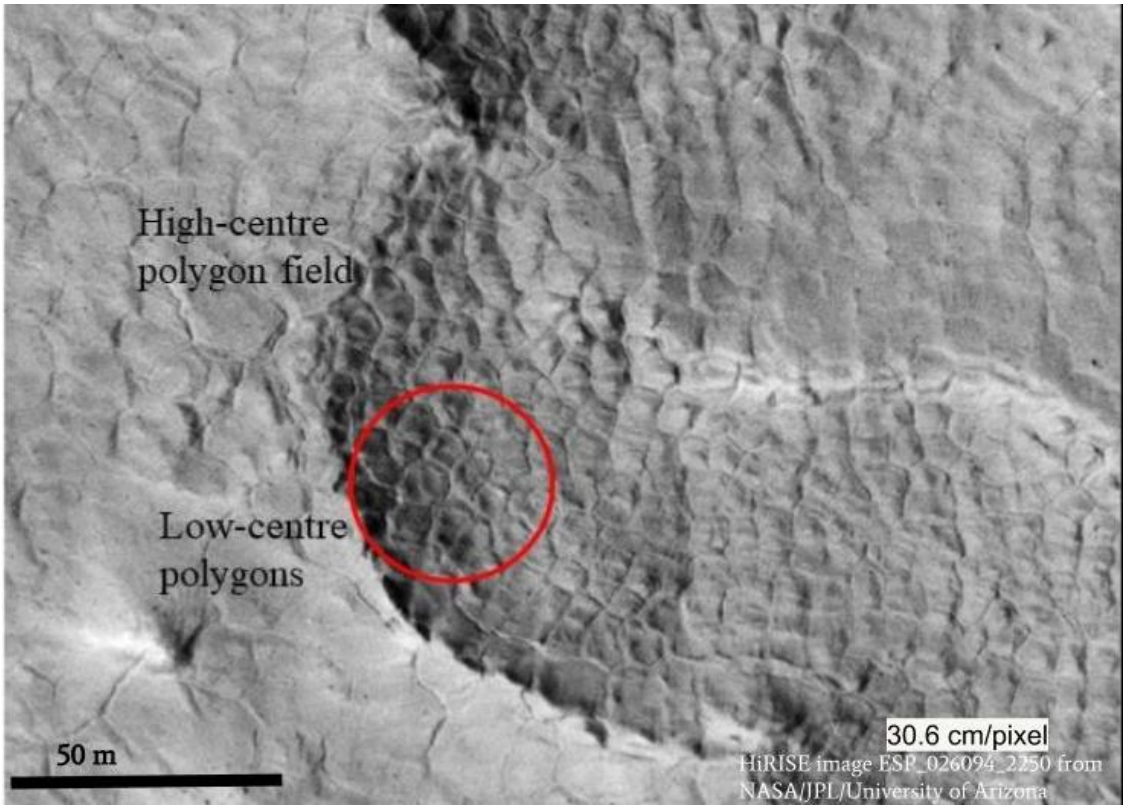

Figure 3.2: A HiRISE image of polygonal terrain in Utopia Planitia, Mars (HiRISE image ESP_026094_2250 from NASA/JPL/University of Arizona).

Future work is especially needed for the Lake Orbiter site which displays significant site-specific variability in polygon morphology. The variations in polygon morphology at Lake Orbiter include polygons differing in size, shape, orthogonality and degree of low-centeredness. There is a noticeable north-south trend in the morphological variations that may be related to grain-size distribution or hydrology of the site and should be explored further. Such variations at a local scale may have more specific implications for future work using this area as a Mars analogue. Similar variations have been observed in HiRISE images of Utopia Planitia where single polygons or small clusters of polygons displaying low-centres are found in larger fields of high-centred polygons (Fig. 3.2) (Soare et al. 2018). Therefore, the factors influencing the variations at a local scale at Lake Orbiter may provide insight into such variations on Mars. More detailed studies of differing polygon morphology that includes the parameters highlighted in this study as well as in studies such as Ulrich et al. (2011) and Brooker et al. (2018) are suggested to provide a more

standardized analysis of polygonal terrain on both Earth and Mars. Such standardized measurements may lead to a deeper understanding of the physical factors affecting polygon morphology across many locations, and how it relates to the concentration and distribution of water ice in the near-subsurface.

3.2 References

Brooker, L.M., Balme, M.R., Conway, S.J., Hagermann, A., Barrett, A.M., Collins, G.S., and Soare, R.J. 2018. Clastic polygonal networks around Lyot crater, Mars: Possible formation mechanisms from morphometric analysis. Icarus, **302**: 386–406.

Dutilleul, P., Haltigin, T.W., and Pollard, W.H. 2009. Analysis of polygonal terrain landforms on Earth and Mars through spatial point patterns. Environmetrics, **20**: 206–220.

French, H.M. 2007. The Periglacial Environment. 3rd ed. John Wiley, Chichester, UK

Haltigin, T.W., Pollard, W.H., Dutilleul, P., and Osinski, G.R. 2012. Geometric evolution of polygonal terrain networks in the Canadian High Arctic: evidence of increasing regularity over time. Permafrost and Periglacial Processes, **23**: 178–186.

Lachenbruch, A.H. 1962. Mechanics of thermal contraction cracks and ice-wedge polygons in permafrost. Geologic Society of America Special Papers, **70**.

Romanovskji, N.N., 1985. Distribution of recently active ice and soil wedges in the USSR. In: Church, M., Slaymaker, O. (Eds.), Field and Theory; Lectures in Geocryology. University of British Columbia Press, Vancouver, pp. 154–165

Soare, R.J., Conway, S.J., Godin, E., Hawkswell, J.E., Osinski, G.R., Bina, A. 2018. Possible ice-wedge polygonization in Utopia Planitia, Mars and its poleward latitudinal-gradient. In Proceedings of the 49th Lunar and Planetary Science Conference, The Woodlands, TX (Abstract #2083).

Ulrich, M., Hauber, E., Herzschuh, U., Härtel, S., and Schirrmeister, L. 2011. Polygon pattern geomorphometry on Svalbard (Norway) and western Utopia Planitia (Mars) using high-resolution stereo remote-sensing data. Geomorphology, **134**: 197–216.

Curriculum Vitae

Name:	Jordan E. Hawkswell
Post-secondary Education and Degrees:	Dalhousie University Halifax, Nova Scotia, Canada 2010-2014 B.Sc. The University of Western Ontario London, Ontario, Canada 2016-2018 M.Sc.
Honours and Awards:	POLAR Northern Scientific Training Program Award 2017
Related Work Experience	Teaching Assistant The University of Western Ontario 2017-2018

Publications:

Hawkswell, J. E., King, D. A., Battler, M. M. and Osinski, G. R. (2017). Documentation of Science and Planning Team Activities for the 2016 CanMARS Sample Return Analogue Mission. 48th Lunar and Planetary Science Conference, The Woodlands, TX, abstract #2398

Hawkswell, J. E., Godin, E., Osinski, G. R., Zanetti, M., and Kukko, A. (2018). Comparative Investigation of Polygon Morphology Within the Haughton Impact Structure, Devon Island with Implications for Mars. 49th Lunar and Planetary Science Conference, The Woodlands, TX, abstract #2899

Bednar, D., Hawkswell, J. E., King, D. Battler, M. M and Osinski, G. R. (2018). Documentation of Science and Planning Deliberation and Decision-Making Process During the CanMars 2016 Mission: Observations and Recommendations for Future Missions. For: Planetary and Space Science. (submitted)